

AD-A128 657

ON THE NUMERICAL ACCURACY OF HOMOGENEOUS SOLID  
PROPELLANT COMBUSTION MODE. (U) ARMY ARMAMENT RESEARCH  
AND DEVELOPMENT COMMAND ABERDEEN PROV.  
M S MILLER ET AL. OCT 82 ARBRL-TR-82425

1/1

UNCLASSIFIED

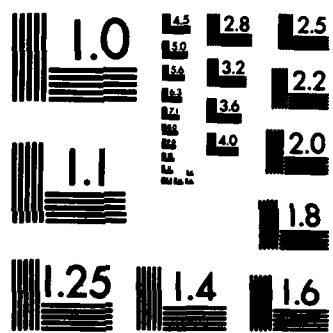
F/G 19/1

NL


END

FILMED

DIC



MICROCOPY RESOLUTION TEST CHART  
NATIONAL BUREAU OF STANDARDS-1963-A

*12*

AD-F300 090  
AD

AD A 120657

TECHNICAL REPORT ARBRL-TR-02425

ON THE NUMERICAL ACCURACY OF  
HOMOGENEOUS SOLID PROPELLANT  
COMBUSTION MODELS

Martin S. Miller  
Terence P. Coffee

DTIC  
SELECTED  
OCT 20 1982  
S H

October 1982



**US ARMY ARMAMENT RESEARCH AND DEVELOPMENT COMMAND**  
**BALLISTIC RESEARCH LABORATORY**  
**ABERDEEN PROVING GROUND, MARYLAND**

Approved for public release; distribution unlimited.

DTIC FILE COPY

82 09 30 003

Destroy this report when it is no longer needed.  
Do not return it to the originator.

Secondary distribution of this report is prohibited.

Additional copies of this report may be obtained  
from the National Technical Information Service,  
U. S. Department of Commerce, Springfield, Virginia  
22161.

The findings in this report are not to be construed as  
an official Department of the Army position, unless  
so designated by other authorized documents.

*The use of trade names or manufacturers' names in this report  
does not constitute endorsement of any commercial product.*

UNCLASSIFIED

SECURITY CLASSIFICATION OF THIS PAGE (When Data Entered)

REPORT DOCUMENTATION PAGE		READ INSTRUCTIONS BEFORE COMPLETING FORM
1. REPORT NUMBER Technical Report ARBRL-TR-02425	2. GOVT ACCESSION NO. <b>AD-A220657</b>	3. RECIPIENT'S CATALOG NUMBER
4. TITLE (and Subtitle) ON THE NUMERICAL ACCURACY OF HOMOGENEOUS SOLID PROPELLANT COMBUSTION MODELS	5. TYPE OF REPORT & PERIOD COVERED FINAL	
	6. PERFORMING ORG. REPORT NUMBER	
7. AUTHOR(s) MARTIN S. MILLER AND TERENCE P. COFFEE	8. CONTRACT OR GRANT NUMBER(s)	
9. PERFORMING ORGANIZATION NAME AND ADDRESS US Army Ballistic Research Laboratory ATTN: DRDAR-BLI Aberdeen Proving Ground, MD 21005	10. PROGRAM ELEMENT, PROJECT, TASK AREA & WORK UNIT NUMBERS 1L16268AH80	
11. CONTROLLING OFFICE NAME AND ADDRESS US Army Armament Research & Development Command US Army Ballistic Research Laboratory (DRDAR-BL) Aberdeen Proving Ground, MD 21005	12. REPORT DATE October 1982	
	13. NUMBER OF PAGES 46	
14. MONITORING AGENCY NAME & ADDRESS (if different from Controlling Office)	15. SECURITY CLASS. (of this report)  UNCLASSIFIED	
	15a. DECLASSIFICATION/DOWNGRADING SCHEDULE	
16. DISTRIBUTION STATEMENT (of this Report) Approved for public release; distribution unlimited.		
17. DISTRIBUTION STATEMENT (of the abstract entered in Block 20, if different from Report)		
18. SUPPLEMENTARY NOTES To be published in Combustion and Flame		
19. KEY WORDS (Continue on reverse side if necessary and identify by block number) Propellant Combustion Models Heat Feedback Calculations Analytic Approximation Numerical Solution		
20. ABSTRACT (Continue on reverse side if necessary and identify by block number) raj Most theoretical treatments of solid propellant combustion assume a highly idealized mechanism: an exothermic surface decomposition reaction followed by a single exothermic gas-phase reaction. Despite its conceptual simplicity this mechanism does not permit an exact solution to the conservation equations. Published combustion models addressing the stated idealization rely on various approximation schemes which have never been tested for accuracy. This report examines the numerical reliability of a number		

DD FORM 1473  
1 JAN 73

EDITION OF 1 NOV 65 IS OBSOLETE

UNCLASSIFIED

SECURITY CLASSIFICATION OF THIS PAGE (When Data Entered)

Unclassified

SECURITY CLASSIFICATION OF THIS PAGE(When Data Entered)

Abstract (Cont'd):

→ 20. of these schemes by direct comparison of model results with accurate numerical integrations of the conservation equations. Four propellant data sets which span a wide range of kinetics parameters were utilized. None of the approximations proved accurate for all the data sets but some models are quite accurate in certain limiting cases. The calculations provide a benchmark against which future models might be tested.

UNCLASSIFIED

SECURITY CLASSIFICATION OF THIS PAGE(When Data Entered)

TABLE OF CONTENTS

	PAGE
LIST OF ILLUSTRATIONS.....	5
I. INTRODUCTION.....	7
II. DESCRIPTION OF PROBLEM AND NUMERICAL SOLUTION.....	7
A. BASIC IDEALIZATION.....	7
B. NUMERICAL SOLUTION.....	9
C. ANALYTIC MODELS USED FOR COMPARISON.....	10
III. RESULTS.....	12
A. FLAME STRUCTURE.....	12
B. HEAT FEEDBACK VS. SURFACE TEMPERATURE.....	12
C. BURNING RATE.....	24
D. TEMPERATURE SENSITIVITY VS. INITIAL TEMPERATURE.....	24
IV. CONCLUSIONS.....	29
REFERENCES.....	37
LIST OF SYMBOLS.....	39
DISTRIBUTION LIST.....	41

Accession For	
NTIS GRA&I	<input checked="" type="checkbox"/>
DTIC TAB	<input type="checkbox"/>
Unannounced	<input type="checkbox"/>
Justification	
By _____	
Distribution/	
Availability Codes	
(Avail and/or	
Dist	Special
A	



## LIST OF ILLUSTRATIONS

FIGURE		PAGE
Fig. 1.	Comparison of numerical (N) and model heat release profiles for the RDX1 data set.....	13
Fig. 2.	Comparison of numerical (N) and model temperature profiles for the RDX1 data set....	14
Fig. 3.	Comparison of numerical (N) and model heat release profiles for the NC3 data set.....	15
Fig. 4.	Comparison of numerical (N) and model temperature profiles for the NC3 data set.....	16
Fig. 5.	Heat feedback vs. surface temperature for NC1 at 1 atm.....	17
Fig. 6.	Heat feedback vs. surface temperature for NC1 at 1000 atm.....	18
Fig. 7.	Heat feedback vs. surface temperature for RDX1 at 1 atm.....	19
Fig. 8.	Heat feedback vs. surface temperature for RDX1 at 1000 atm.....	20
Fig. 9.	Heat feedback vs. surface temperature for NC3 at 1 atm.....	21
Fig. 10.	Heat feedback vs. surface temperature for NC3 at 1000 atm.....	22
Fig. 11.	Heat feedback vs. surface temperature for NC2 at 136 atm.....	23
Fig. 12.	Mass burning rate vs. initial temperature for NC2 at 136 atm.....	25

## I. INTRODUCTION

The mechanism of solid propellant combustion is commonly idealized as a single exothermic pyrolysis reaction occurring at the surface followed by a single exothermic chemical reaction in the gas phase. Additional assumptions, such as constant thermal conductivity, and unit Lewis number, are also usual. The appropriate equations and boundary conditions are derived elsewhere.<sup>1</sup> A comparison of the solution to these equations with experimentally measured burning rates should provide information as to the correctness of the assumed mechanism. In practice one of the difficulties with this line of reasoning (others are discussed in Ref. 2) is that these equations do not have analytic solutions and indeed can sometimes be difficult to solve numerically. Generally this problem has been dealt with by making further simplifications in the equations to obtain a convenient computational algorithm. The object of this paper is to test the accuracy of these algorithms by direct comparison with numerical solutions.

It has previously been shown<sup>1</sup> that most models addressing the stated mechanism can be catalogued by the assumed manner of heat release in the gas-phase. These methods of specifying the heat release are generally appropriate to complementary ranges in the kinetics parameters. Since no general agreement exists on the values of these parameters for any propellant, we have developed several data sets which cover a sufficient range of variation to probe the strengths and weaknesses of all the model algorithms. The reasoning behind these data sets is given in a companion paper<sup>2</sup> but the values are summarized here in Table 1 for convenience.

## II. DESCRIPTION OF PROBLEM AND NUMERICAL SOLUTION

### A. Basic Idealization.

The mechanism used in this study is common to more models than probably any other. Along with the attendant conservation equations, it is thoroughly discussed in Reference 1. In brief, it is assumed that propellant molecules "A" pyrolyze at the solid surface into gaseous products "B" and "C" at the mass burning rate  $M$  ( $\text{gm}/\text{cm}^2\text{s}$ ) which depends on the surface temperature  $T_s$  according to

$$M = M_0 \exp(-E_s/RT_s) \quad (1)$$

(Symbols are identified in the List of Symbols and in Reference 1). This surface reaction is exothermic by an amount  $Q_s$  ( $\text{cal}/\text{gm}$ ). The pyrolysis product B is the reactant for the gas-phase reaction of order  $\nu$ . B is converted by this reaction into non-reactive products C with the release of  $Q_G$  calories per gram of B.

<sup>1</sup>Miller, M.S., "In Search of an Idealized Model of Homogeneous Solid Propellant Combustion," Combustion and Flame, Vol. 46, pp. 51-73, 1982.

<sup>2</sup>Miller, M.S. and Coffee, T.P., "A Fresh Look at the Classical Approach to Solid Propellant Combustion Modeling," to be published in Combustion and Flame.

TABLE I.

	RDX1	NC1	NC2	NC3	T1
$M_O$ (gm/cm <sup>2</sup> sec)	1.035E12	8.0E10	3456	460	1.0E12
$E_s$ (kcal/mole)	47.8	42	10	8	45.0
$Q_s$ (cal/gm)	160	75	53	75	75
$A_G$	2.5E16 (sec <sup>-1</sup> )	2.5E9 (cc/gm sec)	1.44E12 (sec <sup>-1</sup> )	1.2E5 (sec <sup>-1</sup> )	100T (sec <sup>-1</sup> )
$E_G$ (kcal/mole)	46.2	15	54	5	0
$Q_G$ (cal/gm)	460	400	422	350	500
$W_B$ (gm/mole)	222	40	40	40	50
$\nu$	1	2	1	1	1
$m_B^{-0}$	.48	1	1	1	1
$N_2$	6	1.33	1.33	1.33	1
$\rho_s$ (gm/cm <sup>3</sup> )	1.6	1.6	1.55	1.6	1.6

$$\lambda = 2.0E - 4 \text{ cal/cm sec}^\circ\text{K}$$

$$C_p = .35 \text{ cal/gm}^\circ\text{K}$$

In the pyrolysis reaction for every unit mass of A the fraction  $m_B^{-0}$  is converted to B and  $(1-m_B^{-0})$  is converted directly to C. At some temperature T, in the gas, the rate at which B is converted to C is given by

$$R = (m_B \rho)^{\nu} A_G \exp(-E_G/RT) \quad (2)$$

where  $m_B$  is the local mass fraction of B and  $\rho$  is the local mass density of the gas. For every mole of B which reacts  $N_2$  moles of C are produced.

### B. Numerical Solution.

The linear burning rate  $r$  is to be calculated for a semi-infinite block of propellant whose surface is situated normal to the  $x$  axis. Because the propellant is homogeneous, the burning is one-dimensional. Two levels of approximation to the conservation equations are discussed in Reference 1. The more general of the two is discussed here (termed Level I in Ref. 1).

The method used to obtain a burning rate in this paper has been discussed schematically in Reference 1. First the conductive heat feedback,  $\phi_G$ , from the gas phase to the surface of the solid is computed numerically for many values of  $T_s$  at a given pressure. A value for  $T_s$  is then sought for which  $\phi_G$  is equal to the heat flux,  $\phi_s$ , required by the solid to maintain a mass regression rate  $M$  when the initial temperature is  $T_0$ , i.e.,

$$\phi_s = MC_p (T_s - T_0 - Q_s/C_p). \quad (3)$$

By using this method the numerical functions  $\phi_G(T_s, P)$  do not depend on either  $Q_s$  or  $T_0$ .

The gas-phase equations are solved by a computer code designed to handle premixed, laminar, one-dimensional flames involving elementary chemistry.<sup>3,4</sup> This code is based on the package PDECOL developed by Madsen and Sincovec<sup>5</sup> to solve sets of second order partial differential equations using finite element techniques.

Although the equation governing  $m_B$  can be eliminated using the unit Lewis number assumption, both the  $m_B$  and the  $T$  equations are integrated by the code. The self-consistency of the two solutions can then be checked, as will be explained (Eq. 4).

<sup>3</sup>Coffee, T.P. and Heimerl, J.M., "A Method for Computing the Flame Speed for a Laminar, Premixed, One Dimensional Flame," Ballistic Research Laboratory Technical Report ARBRL-TR-02212, January 1980. (AD A082803)

<sup>4</sup>Coffee, T.P., "A Computer Code for the Solution of the Equations Governing a Laminar, Premixed, One Dimensional Flame," Ballistic Research Laboratory Memorandum Report No. ARBRL-MR-03165, April 1982. (AD A114041)

<sup>5</sup>Madsen, N.K. and Sincovec, R.F., "PDECOL, General Collocation Software for Partial Differential Equations," ACM TOMS, Vol. 5, pp. 326-351, 1979.

The basic numerical procedure is to work with the time dependent equations using arbitrary starting profiles for  $m_B$  and  $T$ . The cold boundary condition is just  $T=T_s$ . For the mass fraction equation it is<sup>1</sup>

$$m_B^{+0} - \frac{\rho D}{M} \left( \frac{\partial m_B}{\partial x} \right)_{+0} = m_B^{-0},$$

which expresses the required continuity of B mass flux across the boundary. The first derivatives of  $m_B$  and  $T$  are taken to be zero at the hot boundary. Numerically the hot boundary was chosen sufficiently distant from the surface that the  $m_B$  and  $T$  profiles were essentially unaffected by its location. These boundary conditions were previously used to model burner stabilized flames.<sup>4</sup>

The equations are integrated in time until the steady state solution is reached. Since a finite element code is used, the solution profiles are represented by piecewise polynomials and the temperature gradient at the surface is available. As a check the heat feedback is also calculated by the formula

$$\phi_G = Q_G M (m_B^{-0} - m_B^{+0}) \quad (4)$$

which follows from the unit Lewis number assumption.

The steady state solution is usually quickly reached, taking on the order of a second on a CDC 7600. The exception is when  $M$  becomes so large (due to high  $T_s$ ) that the flame is blown far from the surface. This strong convective flow allows little heat to be conducted back to the solid. As a result the flame is barely stabilized and tends to oscillate before finally approaching the steady state.

As a partial check on the code, it was run on a test data set (T1) for which an exact analytic solution exists (Eq. 31 of Ref. 1). The numerical solution proved accurate to within a small fraction of a percent except when  $T_s$  became large enough so that the heat feedback was negligibly small. Even there the numerical solution was good to a few percent (and could be improved by using a finer grid). In the subsequent figures the numerical computations will be denoted by N.

### C. Analytic Models Used for Comparison

Most of the models which deal with our assumed mechanism have been recently reviewed and classified into one of three idealizations of the gas-phase heat release.<sup>1</sup> The constant temperature reaction rate (CTRR) approach should apply in the limit of very low  $E_G$ . The quasi-constant heat release (QCHR) model<sup>1</sup> might pertain to moderate values of  $E_G$  whereas the delta function heat release (DFHR) models would be appropriate to very high  $E_G$ . We shall in this paper compare our numerical calculations to the following specific models in each of these classes.

A solution to  $\phi_G$  under the CTRR assumption is not available for  $\nu=2$  in a Level I (diffusion not neglected) treatment<sup>1</sup>; therefore, Equation (33) of Reference 1 is used to compute  $\phi_G$  for the NCl data set. (Eq. 31 of Ref. 1 is used for the  $\nu=1$  cases). A comparison of the solutions with and without

diffusion for the  $\nu=1$  cases shows that the burning rate is not greatly affected by this assumption so long as the solution value of  $T_s$  lies to the right of the peak in the  $\phi_G(T_s)$  curve. For example, Fig. 5 suggests that the use of the no-diffusion  $\phi_G$  is probably justified for  $T_0$  greater than about  $300^\circ\text{K}$ .

It became apparent during the course of this work that, while the QCHR model  $\phi_G$  gives good results for  $\phi_G$  at high  $T_s$  for some cases, at sufficiently low  $T_s$  the model  $\sigma_G$  exceeds the maximum possible heat feedback ( $Q_G m_B^{-0}$ ). This occurs because at low  $T_s$  the characteristic transport distance ( $\lambda/MC_p$ ) becomes so large (as  $M$  diminishes) that the integrated heat release exceeds  $Q_G m_B^{-0}$ . This problem is easily corrected by assuming a constant heat release,  $q_0$ , only for  $x < x_1$  where  $x_1$  is chosen by the energy conservation requirement

$$Q_G m_B^{-0} = \int_0^{x_1} q_0 dx$$

Thus we have the "constant heat release" (CHR) model given by

$$\phi_G = \frac{\lambda q_0}{MC_p} [1 - \exp(-MC_p x_1 / \lambda)] \quad (5)$$

which will be used in the present paper (cf. Eq. (46) of Reference 1). At high  $T_s$  the QCHR and CHR results for  $\phi_G$  merge. The unknown value of  $m_B^{-0}$  in  $q_0$  is found by requiring self-consistency between Equations (4) and (5).

In Reference 1 it was argued that the BDP monopropellant model<sup>6</sup>, although a delta function model, is likely to overestimate  $\phi_G$  in the limit of high  $E_G$  because of an improper choice for the flame standoff distance.<sup>7</sup> This assessment is borne out in the calculations to follow. Fortunately there does exist an accurate high  $E_G$  theory which was advanced by Williams<sup>8</sup> and elaborated by Buckmaster, et al.<sup>9</sup> The theory is based on the asymptotic analysis of Bush and Fendell<sup>10</sup> for laminar gas flames. In our notation the burning rate<sup>9</sup> for general reaction orders is given by

$$M^2 = \frac{2\nu! \lambda P^\nu A_G R^{\nu+1} C_p^\nu T_f^{2(\nu+1)}}{(E_G Q_G m_B^{-0})^{\nu+1}} \left(\frac{\bar{W}}{RT_f}\right)^\nu \exp(-E_G/RT_f) \quad (6)$$

In this paper we shall designate the theory by A.

<sup>6</sup> Beckstead, M.W., Derr, R.L., and Price, C.E., "The Combustion of Solid Monopropellants and Composite Propellants," *Thirteenth Symposium (International) on Combustion, The Combustion Institute*, pp. 1047-1056, 1971.

<sup>7</sup> Hermance, C.E., "A Model of Composite Propellant Combustion Including Surface Heterogeneity and Heat Generation," *AIAA Journal*, Vol. 4, pp. 1629-1637, 1966.

<sup>8</sup> Williams, F.A., "Quasi-Steady Gas-Flame Theory in Unsteady Burning of a Homogeneous Solid Propellant," *AIAA Journal*, Vol. 11, pp. 1328-1330, 1973.

<sup>9</sup> Buckmaster, J.D., Kapila, A.K., and Ludford, G.S.S., "Linear Condensate Deflagration for Large Activation Energy," *Acta Astronautica*, Vol. 3, pp. 593-614, 1976.

<sup>10</sup> Bush, W.B. and Fendell, F.E., "Asymptotic Analysis of Laminar Flame Propagation for General Lewis Numbers," *Comb. Sci. Tech.*, Vol. 1, pp. 421-428, 1970.

### III. RESULTS

In this section we shall first show how the model heat release and temperature profiles compare with the numerical ones. The comparison is then extended to the heat feedback functions  $\phi_G(T_s, P)$ , the burning rates  $M(P)$ , and finally the temperature sensitivities  $\sigma_p(T_0)$ .

#### A. Flame Structure

Sample comparisons are made in Figs. 1-4 for a high  $E_G$  data set (RDX1) and one with low  $E_G$  (NC3). In both cases the conditions of pressure and initial temperature are 1000atm and 300°K. It is clear that all of the models give very simplistic representations of the heat release ( $q(x)$ ) profiles (Figs. 1 and 3). In Fig. 1 the tendency of the BDP model to underestimate the flame standoff distance<sup>1</sup> for high activation energy is evident. The high activation energy case (Fig. 2) causes the greatest divergence in predicted temperature profiles. The asymptotic theory does quite well, however, at points near the surface. As expected the CHR and CTRR models give significantly better temperature profiles than the flame sheet models for the low activation energy case (Fig. 4).

#### B. Heat Feedback vs. Surface Temperature

Figures 5-11 display the numerical and model values of heat feedback (i.e.,  $\lambda \frac{dT}{dx} \Big|_{x=+0}$ ) as a function of surface temperature for the model propellants. At sufficiently low  $T_s$  all of the models predict  $\phi_G$  to approach the maximum value, i.e.,  $Q_G M_B^{-0}$ . In this limit the bulk of the energy release takes place close (compared with  $\lambda/MC_p$ ) to the surface. Increasing  $T_s$  promotes two competing effects. The gas reaction is accelerated tending to increase  $\phi_G$ , but  $M$  also increases by the pyrolysis law tending to blow the "flame" further away from the surface and reducing the effectiveness of energy release at any given distance from the surface (see the discussion of Eq. (6) in Ref. 1). Eventually the latter processes dominate and  $\phi_G$  decreases with  $T_s$ .

Also shown in these figures is  $\phi_s(T_s)$  computed by Eq. (3) for  $T_0=300^\circ\text{K}$ . The intersection of  $\phi_s(T_s, T_0)$  and  $\phi_G(T_s, P)$  occurs at the value of  $T_s$  pertinent to the conditions  $(T_0, P)$ . With this solution value of  $T_s$  one can compute the burning rate via Eq. (1).

An important feature to notice in these figures is that the CHR model gives the correct value of  $\phi_G$  in the high  $T_s$  limit. (The CHR and QCHR models are identical in this limit). Although the solution to  $\phi_s = \phi_G$  can always be forced to occur in this region by considering a sufficiently high value of  $T_0$ , the fractional heat feedback ( $\frac{\phi_G}{Q_G M_B^{-0}}$ ) may be so small there that the gas phase processes no longer affect the burning rate.

Another interesting feature is the way that the BDP model exhibits similarities to both the asymptotic (A) and CTRR solutions. This results from the BDP model using the delta function (high  $E_G$ ) formalism but with a flame standoff which is appropriate to the low  $E_G$  limit. (See discussion in Section IIIB of Ref. 1).

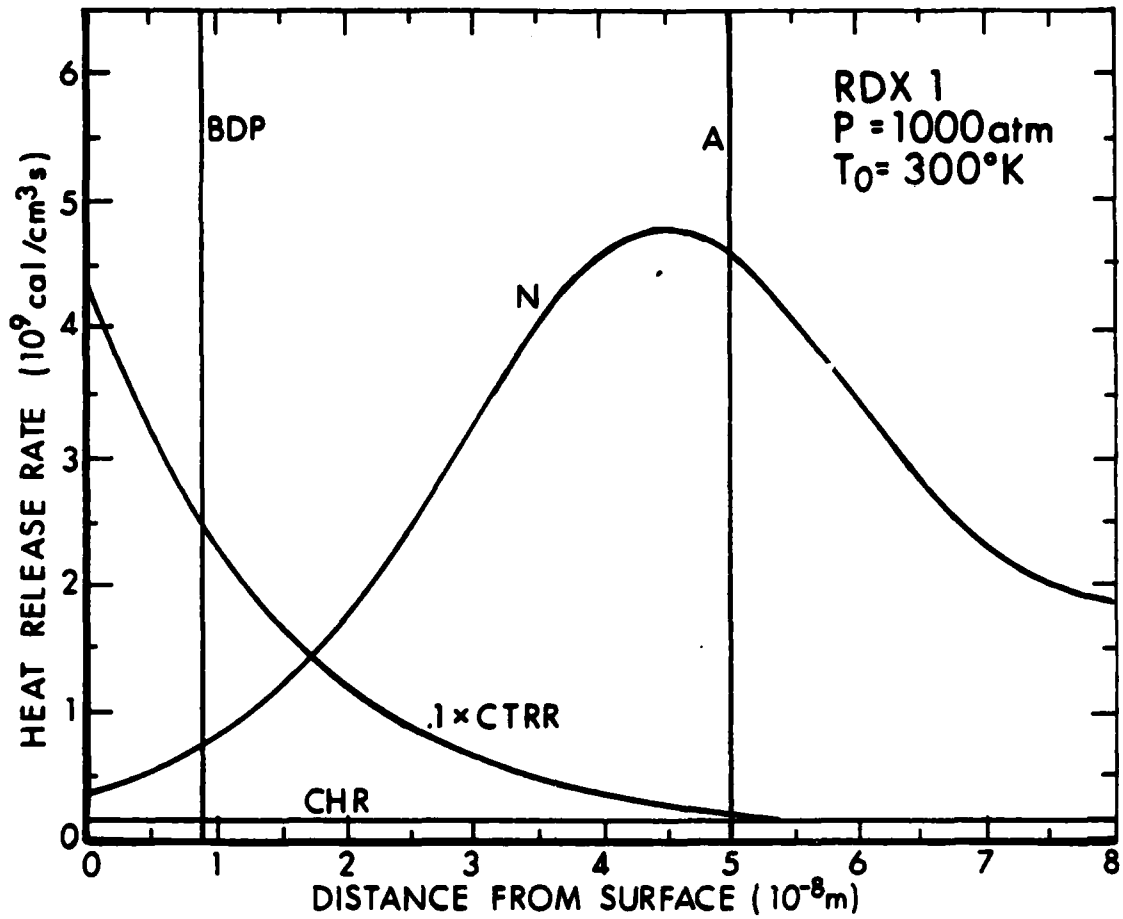


Fig. 1. Comparison of numerical (N) and model heat release profiles for the RDX1 data set.

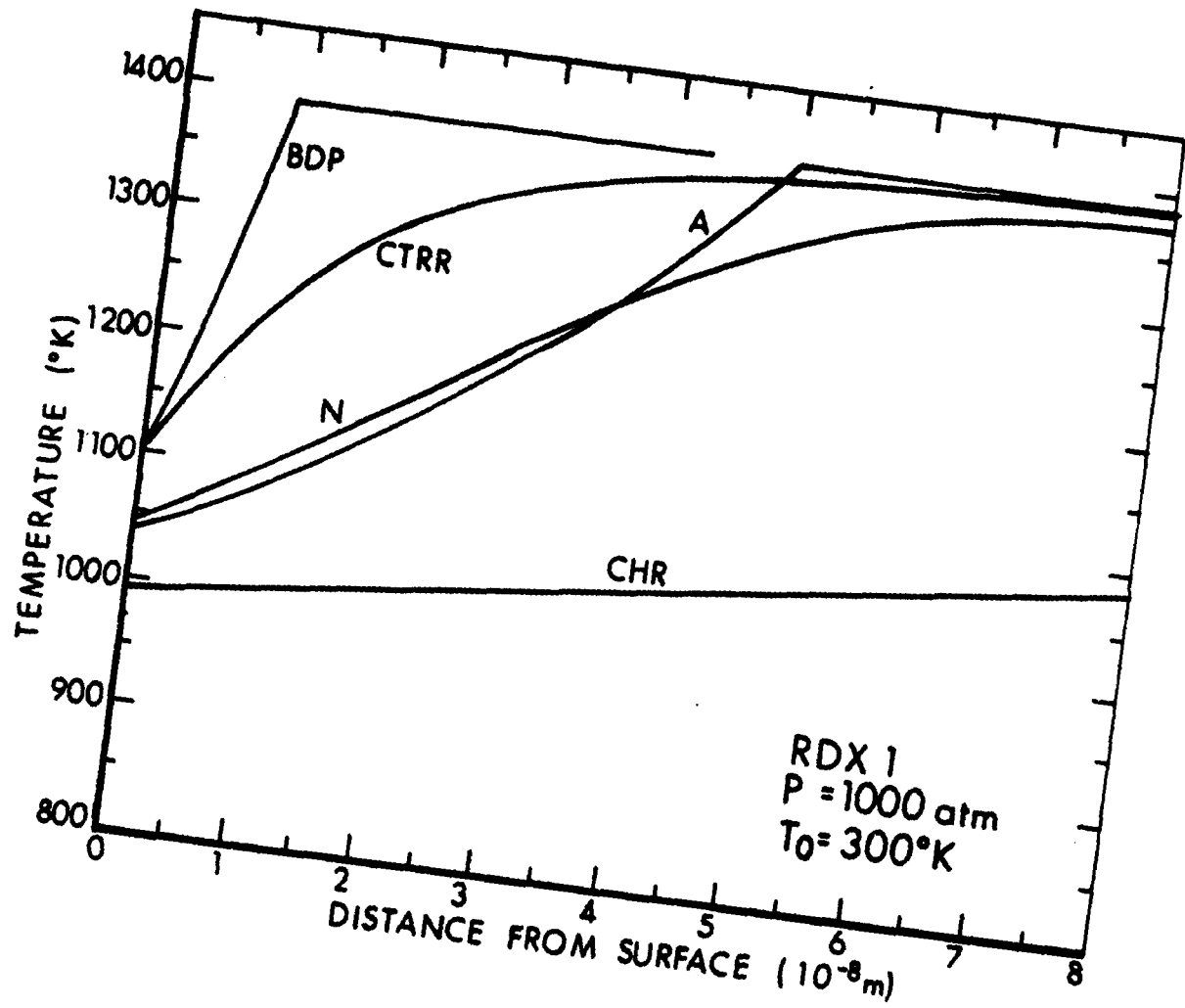


Fig. 2. Comparison of numerical (N) and model temperature profiles for the RDX1 data set.

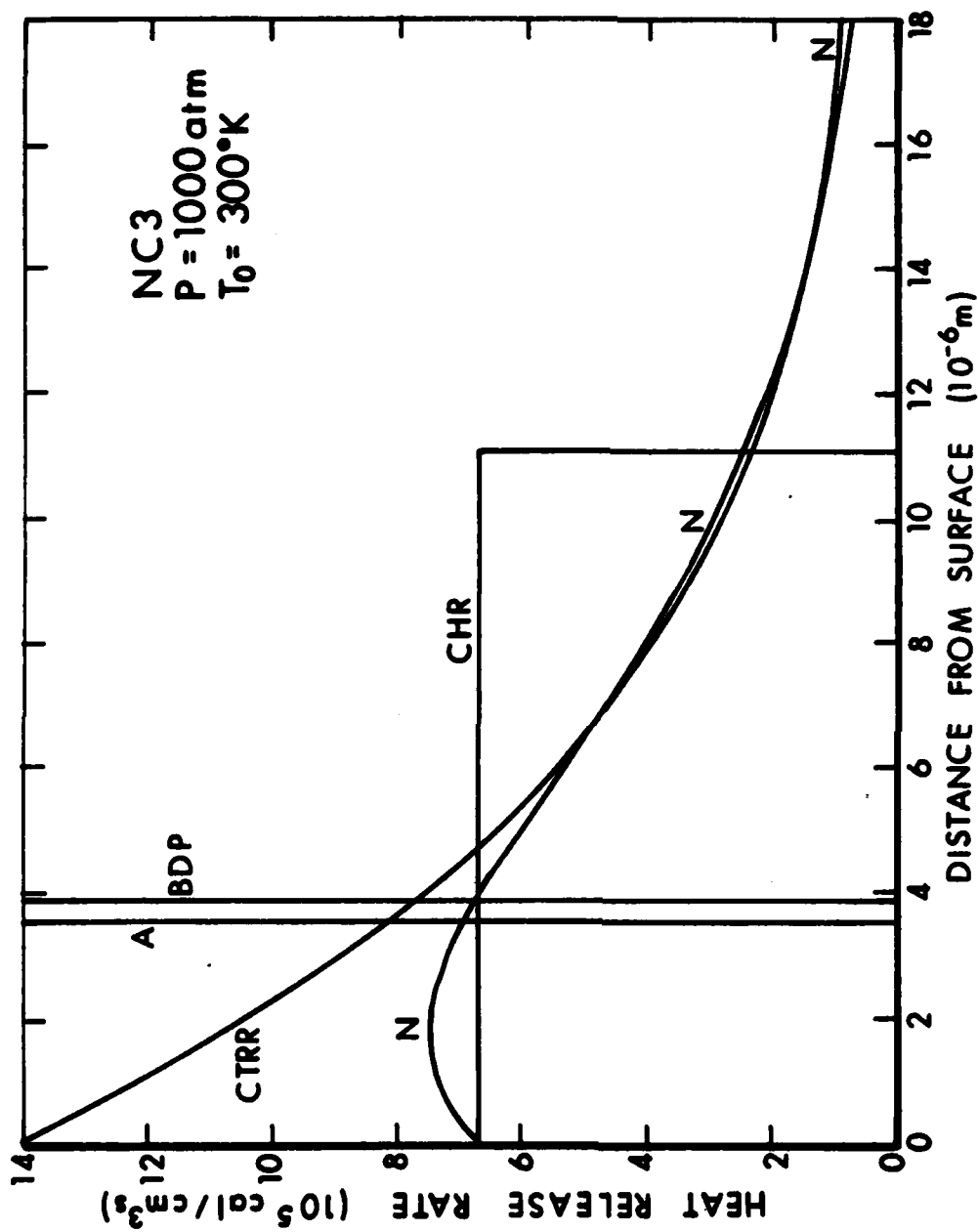


Fig. 3. Comparison of numerical (N) and model heat release profiles for the NC3 data set.

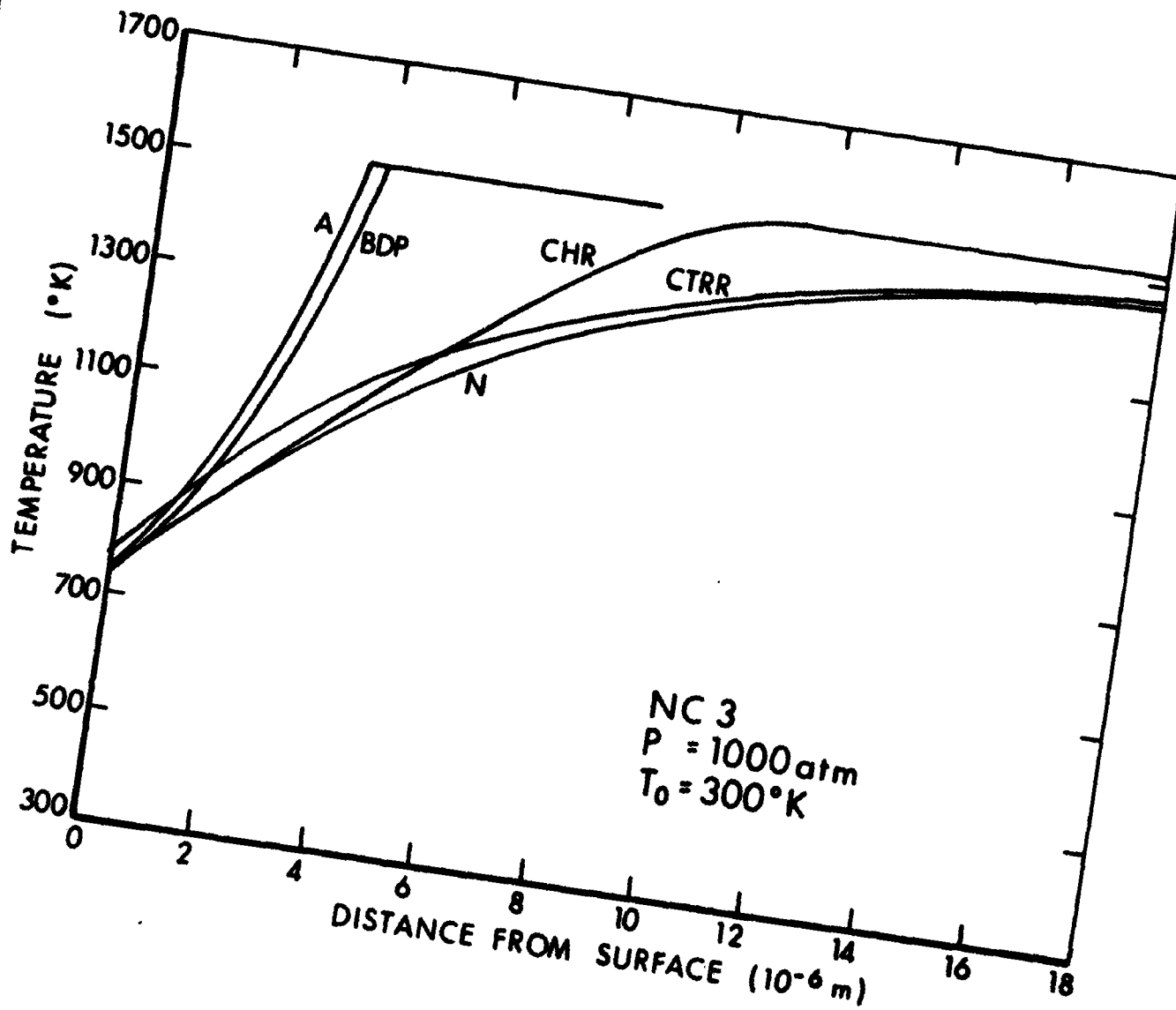


Fig. 4. Comparison of numerical (N) and model temperature profiles for the NC3 data set.

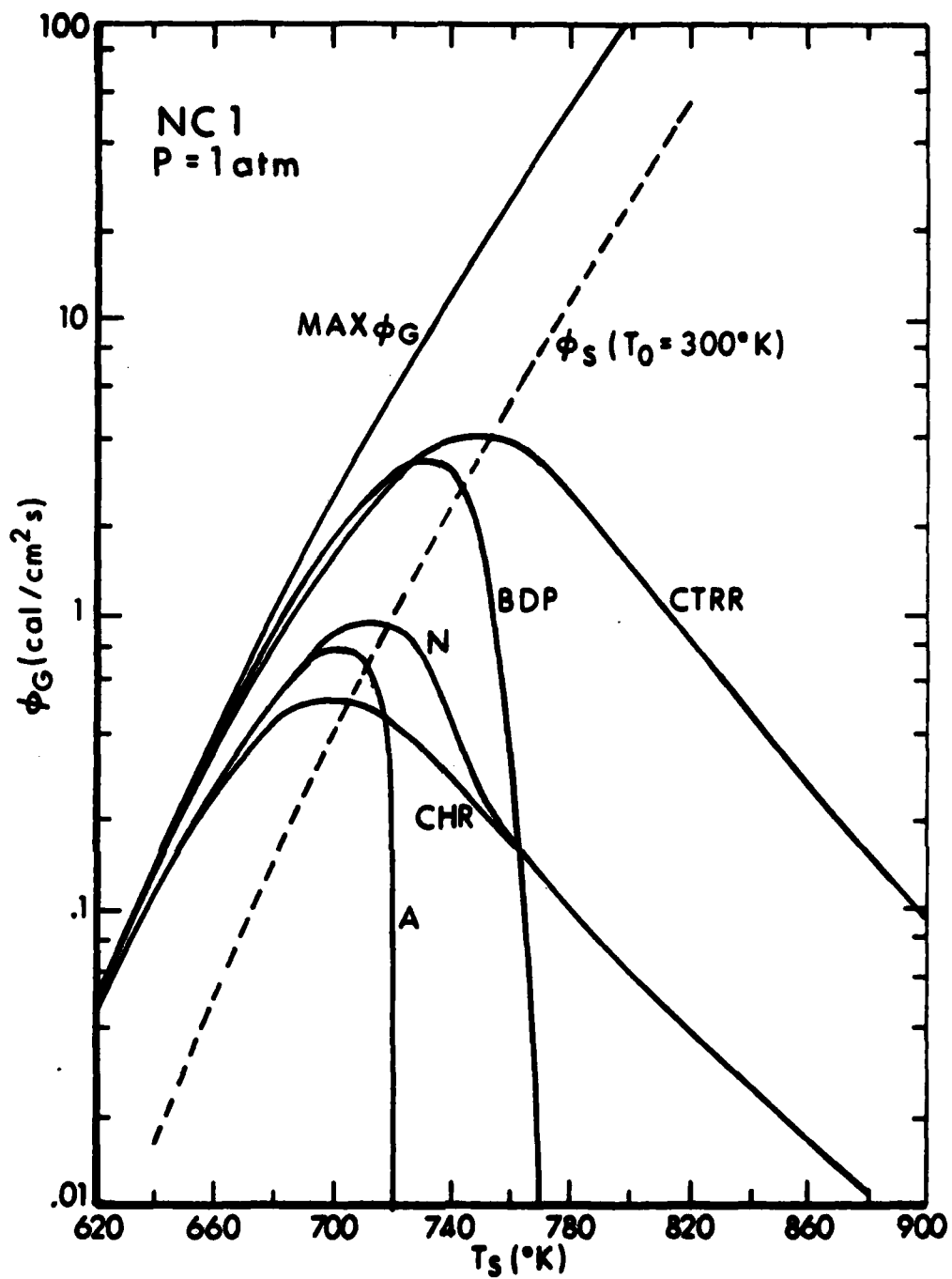


Fig. 5. Heat feedback vs. surface temperature for NC1 at 1 atm.

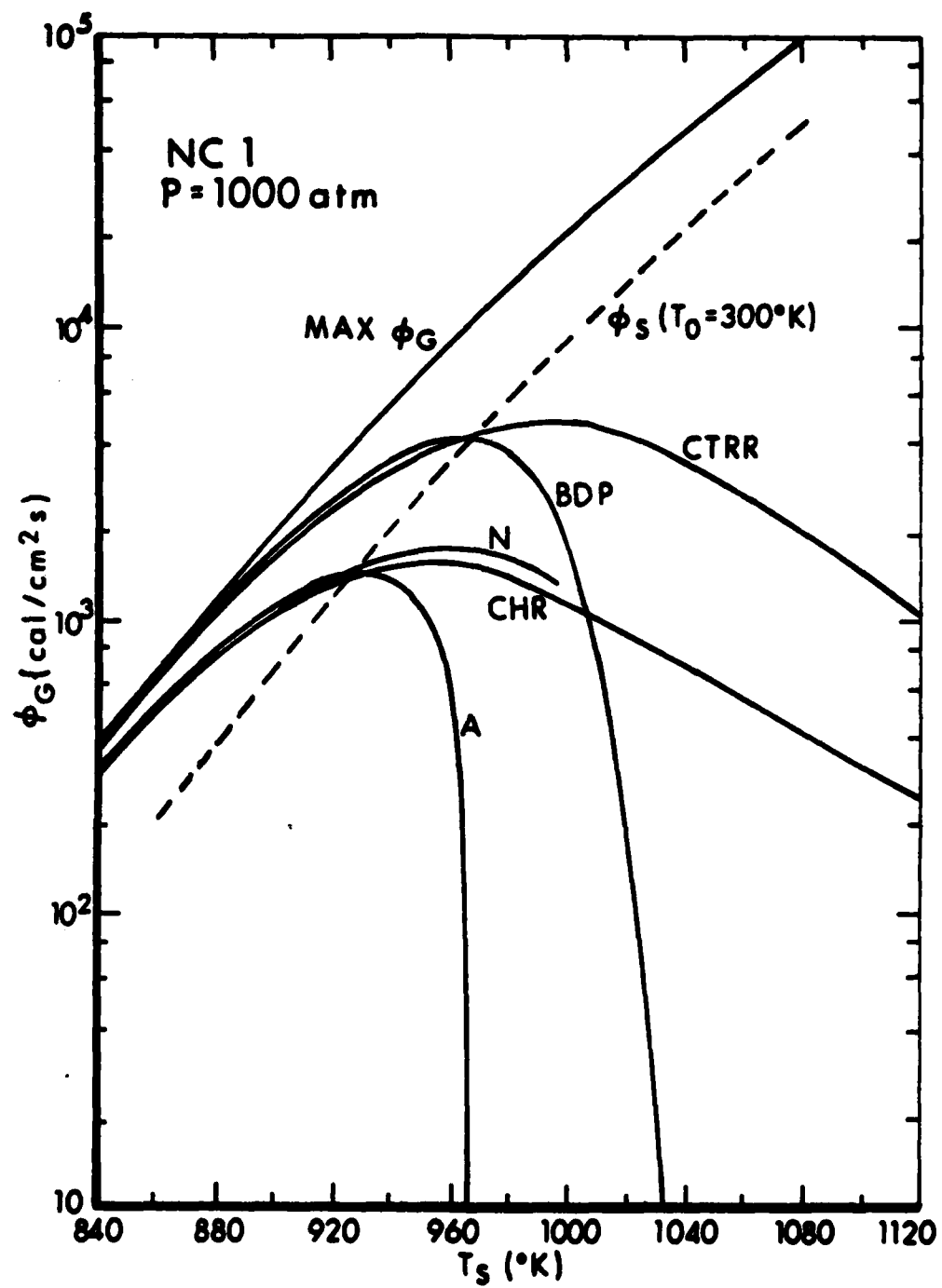


Fig. 6. Heat feedback vs. surface temperature for NC1 at 1000 atm.

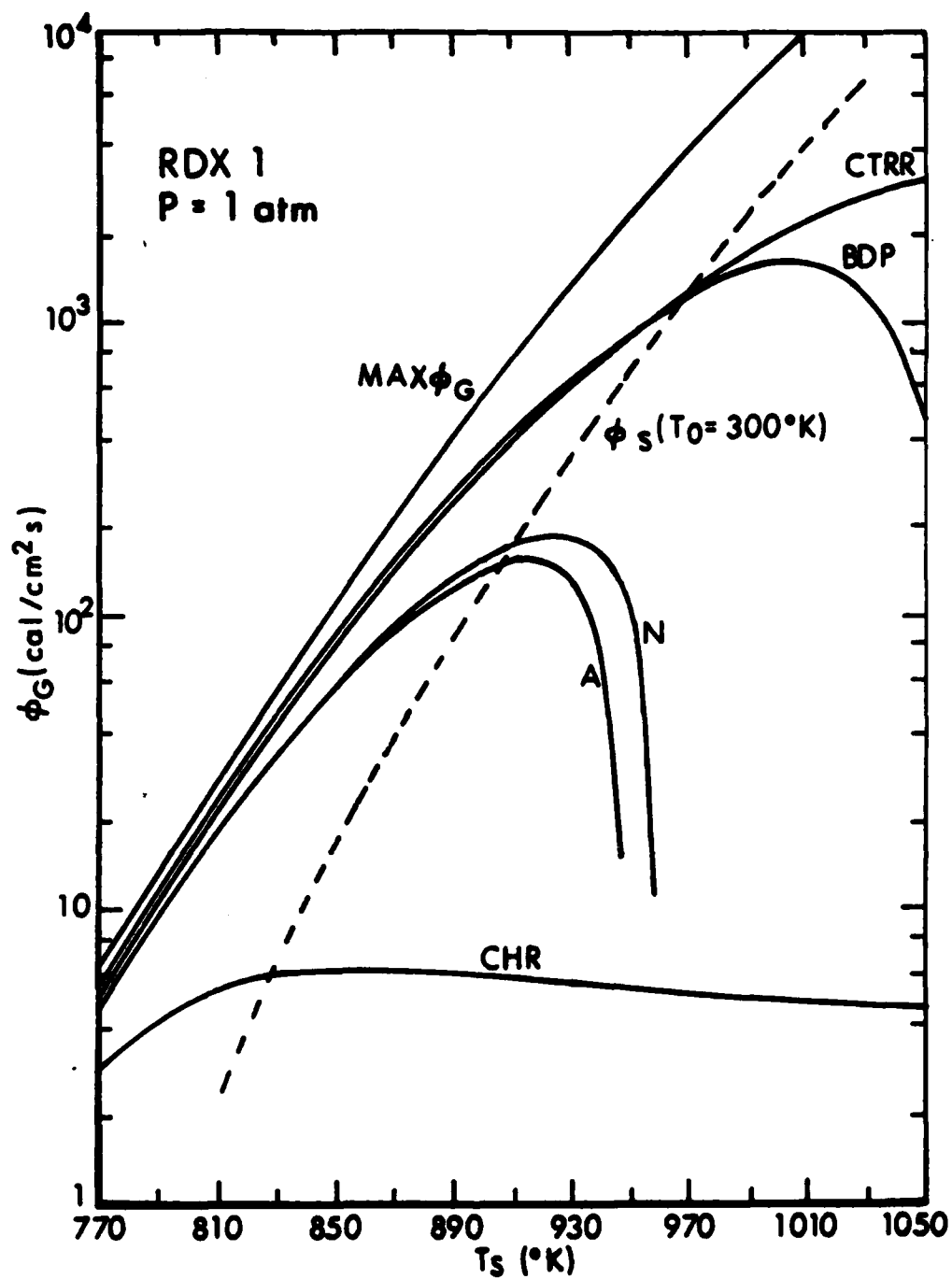


Fig. 7. Heat feedback vs. surface temperature for RDX1 at 1 atm.

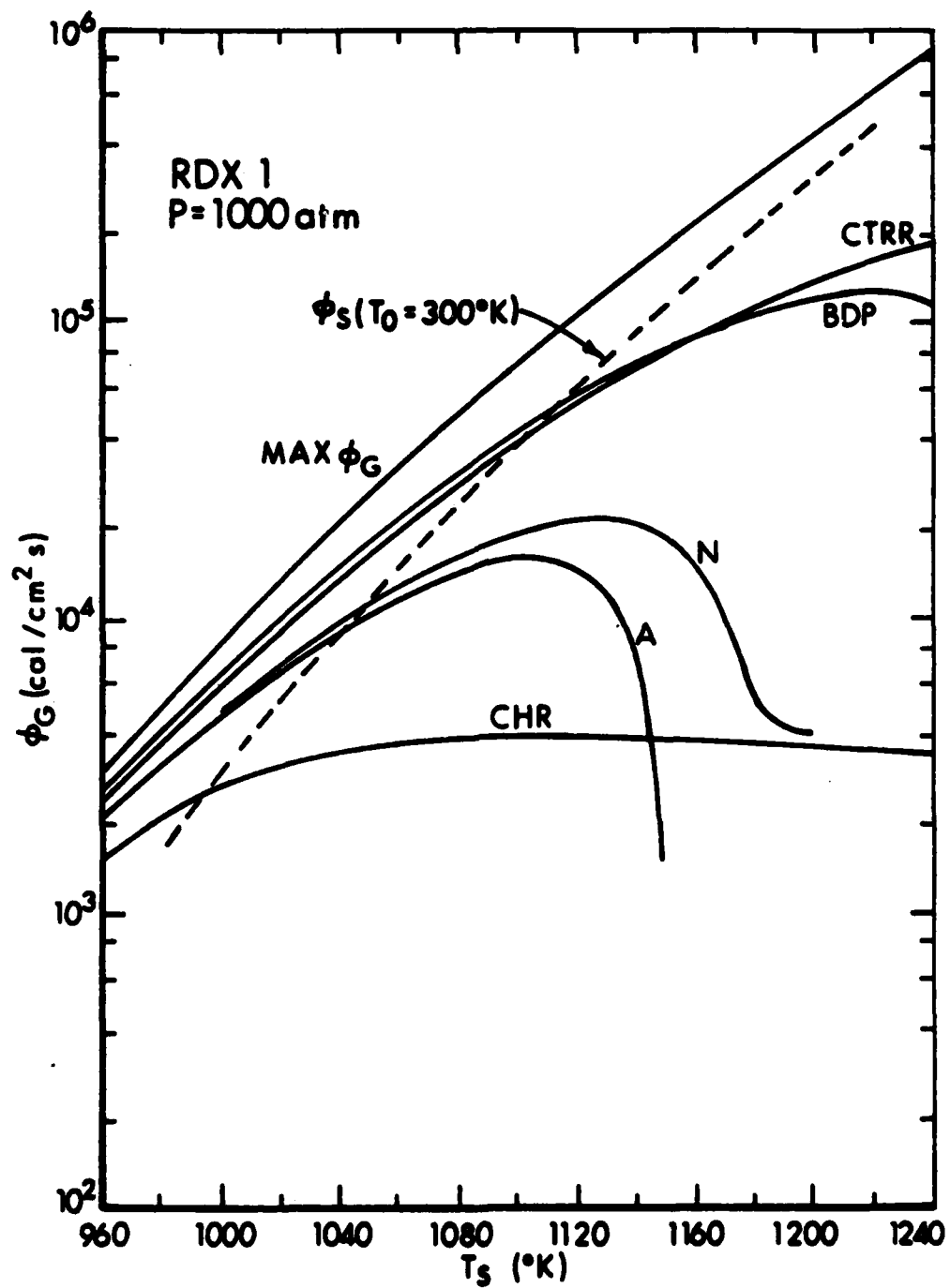


Fig. 8. Heat feedback vs. surface temperature for RDX1 at 1000 atm.

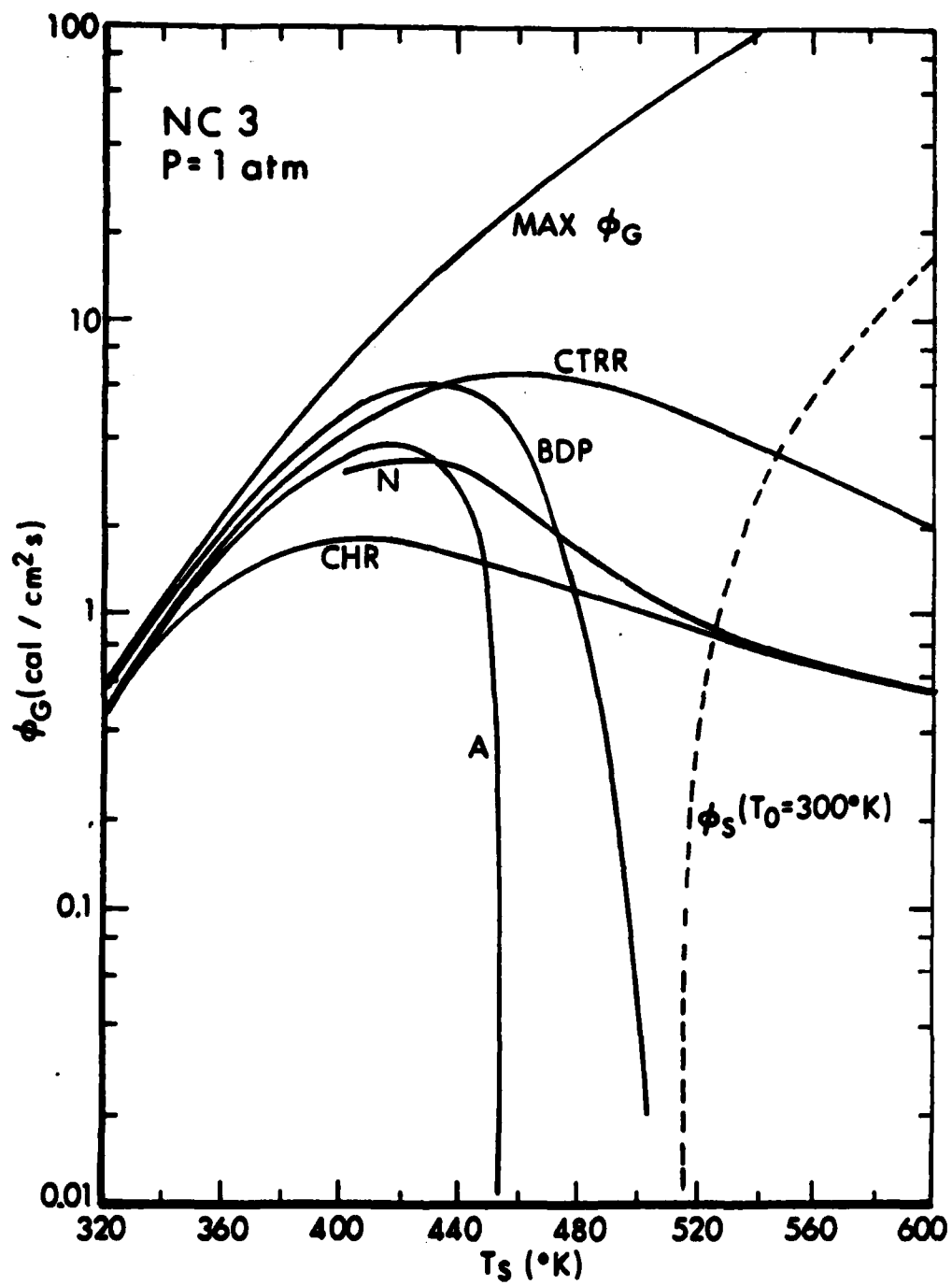


Fig. 9. Heat feedback vs. surface temperature for NC3 at 1 atm.

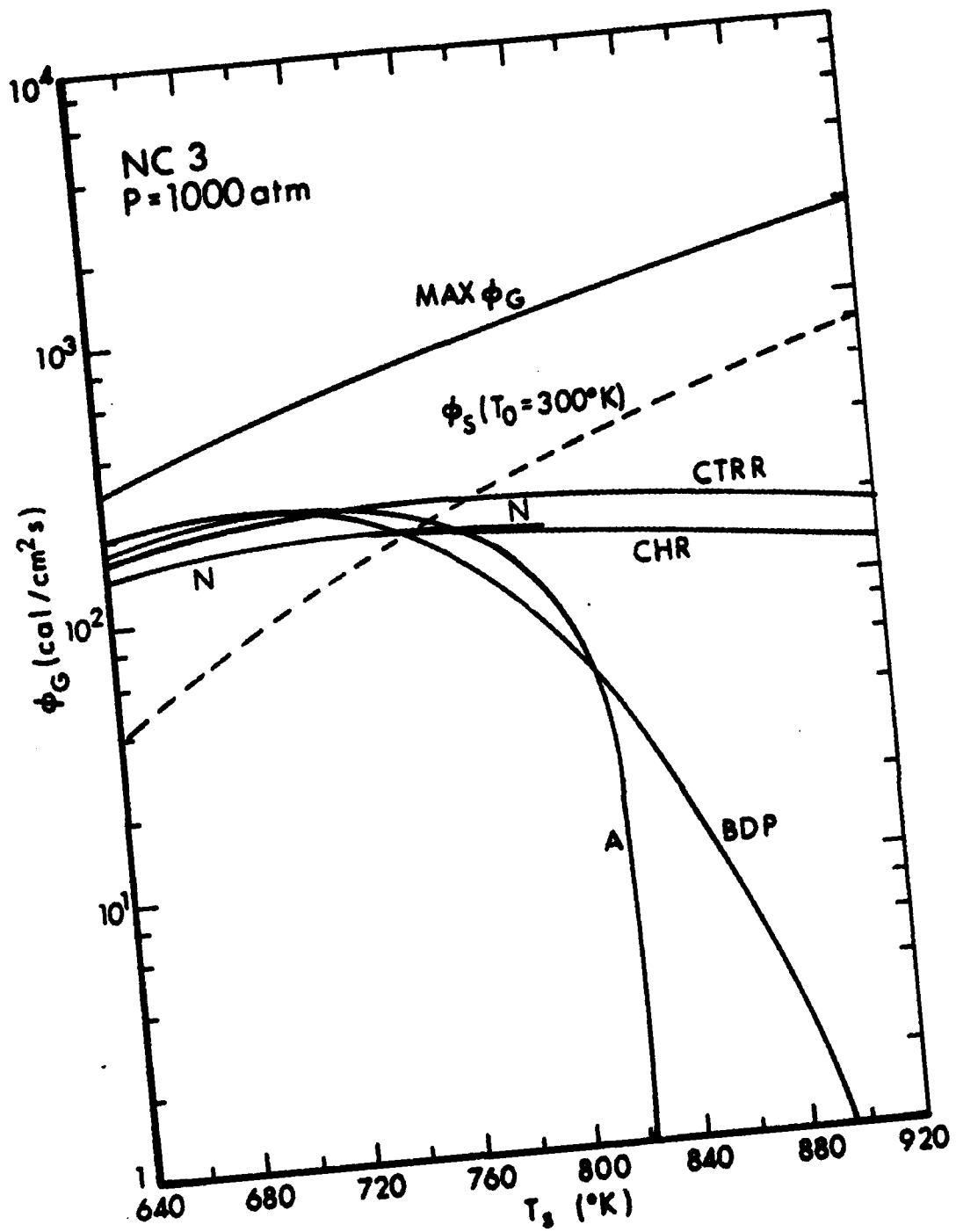


Fig. 10. Heat feedback vs. surface temperature for NC3 at 1000 atm.

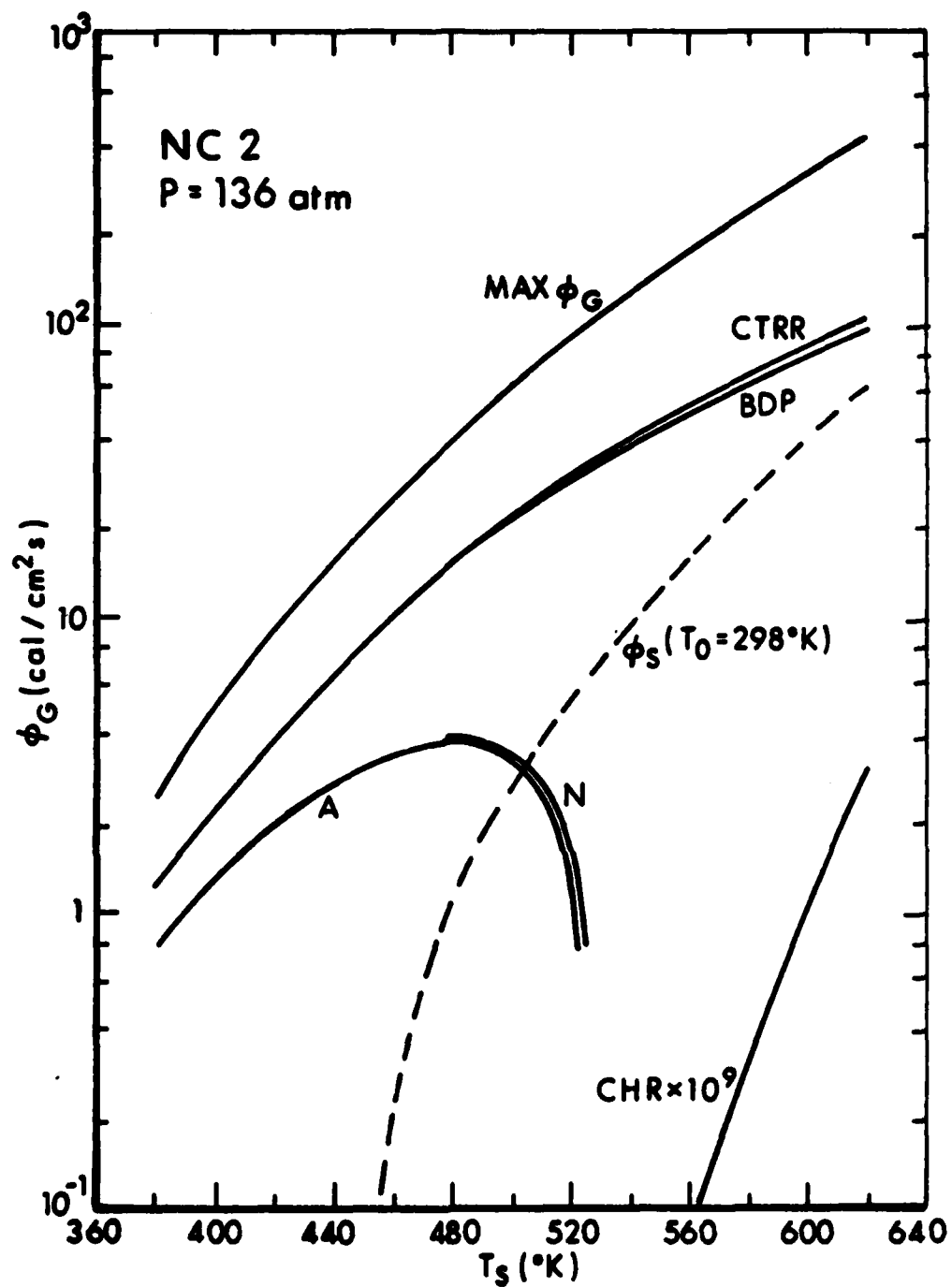


Fig. 11. Heat feedback vs. surface temperature for NC2 at 136 atm.

In general the CTRR approximation is the poorest and is most notably so in the high  $T_s$  region. In this portion of the curve the neglect of diffusion has almost no effect on the numerical value of  $\phi_G$  since  $\frac{R_0}{M^2}$  is small there. (See Section IIIA of Ref. 1).

Finally, Fig. 11 gives good evidence that the asymptotic theory is numerically accurate in the high  $E_G$  limit. The approach to this limit is also evident in Figs. 7 and 8. The asymptotic theory, in fact, does quite well generally although Fig. 9 and high  $T_0$  cases in Figs. 5-8 are exceptions.

In short it is clear that no single combustion model that we have considered can be relied upon for even approximate results under all conditions of  $T_0$  and  $P$  for any set of propellant data.

### C. Burning Rate

The burning rate as a function of initial temperature for the NC2 data set is shown in Fig. 12 at a pressure of 136 atm. The NC2 data set is obtained<sup>2</sup> by a fit of the BDP model to double-base propellant burning rates. However it is clear that the BDP model is particularly inaccurate for the parameters obtained by this fit, overestimating the numerical rate by an order of magnitude. Note that only the asymptotic theory gives good accuracy for this flame-sheet case.

Figures 13, 14, and 15 indicate that, for the most part, the pressure index (exponent) is slightly less than  $\sqrt{2}$  and that the model algorithms approximate this value fairly well. Eq. (61) of Reference 1, which connects the pressure index with  $E_s$  and  $E_G$ , is found to be inaccurate for values other than  $\sqrt{2}$ . The absolute accuracy of  $M$  depends rather strongly on the parameters of the data set. In general the asymptotic theory does best at the highest  $E_G$  (RDX1) and the CHR model does best at the lowest  $E_G$  (NC3). As expected from the discussion of Figures 5-11, the BDP model leads to an overestimate of the burning rate for high  $E_G$ . All of the burning rates in Figs. 8-10 are computed for an initial propellant temperature of 300°K. We note also that the burning rates are computed only at 1, 10, 100, 1000 atm. For clarity, straight lines are used to connect these points.

### D. Temperature Sensitivity vs. Initial Temperature

The temperature sensitivity at constant pressure,  $\sigma_p$ , is defined by

$$\sigma_p \equiv \left( \frac{d \ln M}{dT_0} \right)_p \quad (7)$$

Like the pressure sensitivity ( $\equiv \frac{d \ln M}{d \ln P}$ ) its usefulness lies in the fact that it is nearly constant over variable ranges of practical concern. Though nearly constant,  $\sigma_p$  has nonetheless been observed<sup>2</sup> to increase generally with increases

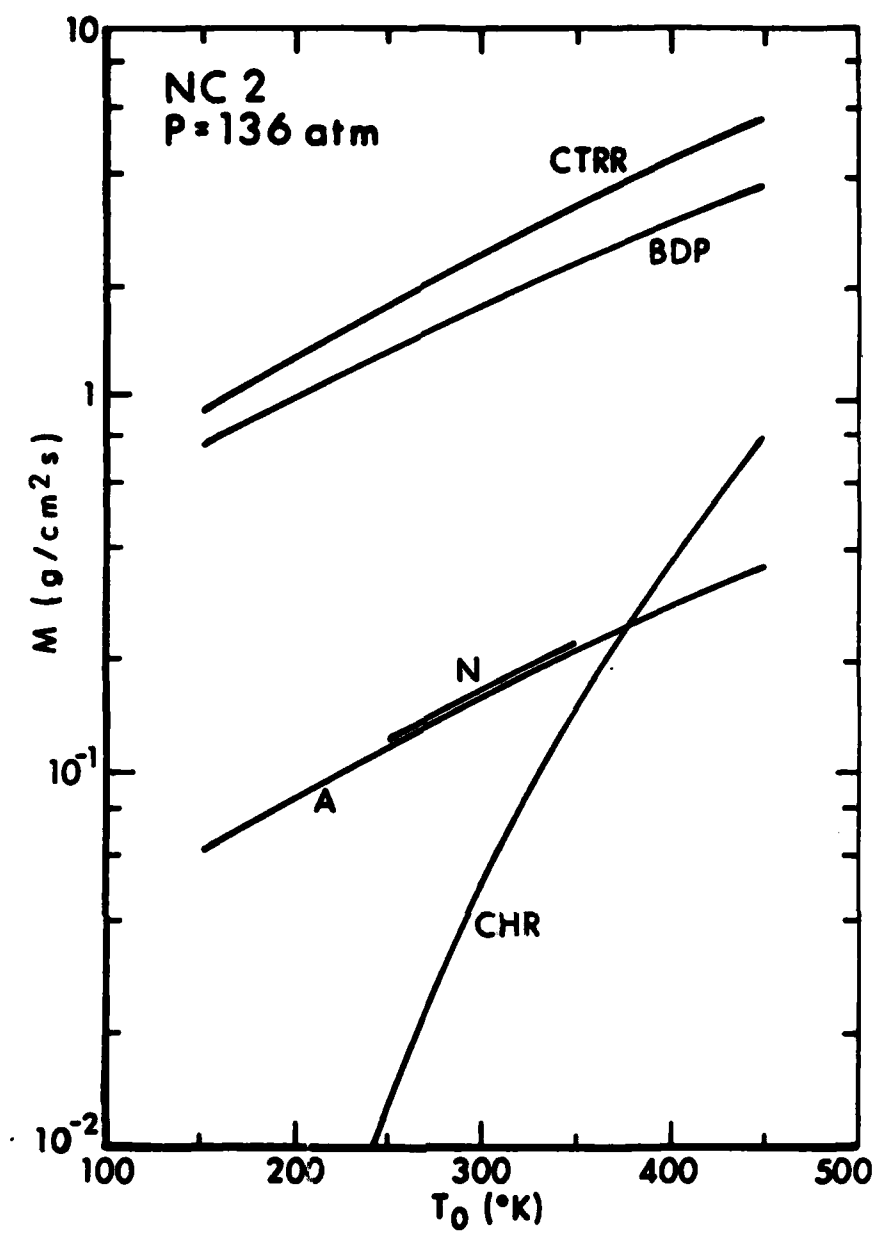


Fig. 12. Mass burning rate vs. initial temperature for NC2 at 136 atm.

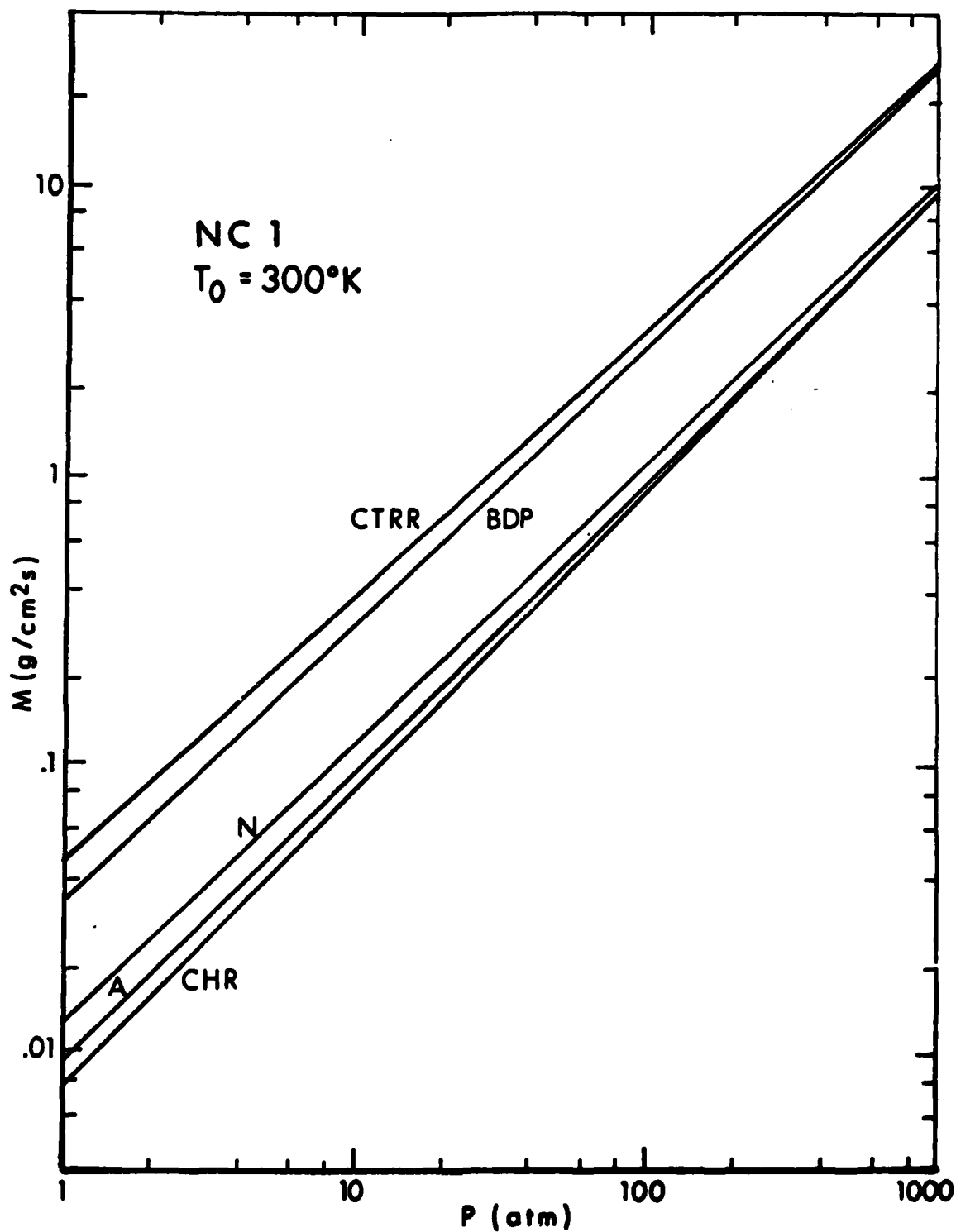


Fig. 13. Mass burning rate vs. pressure for NC1 initially at 300°K.

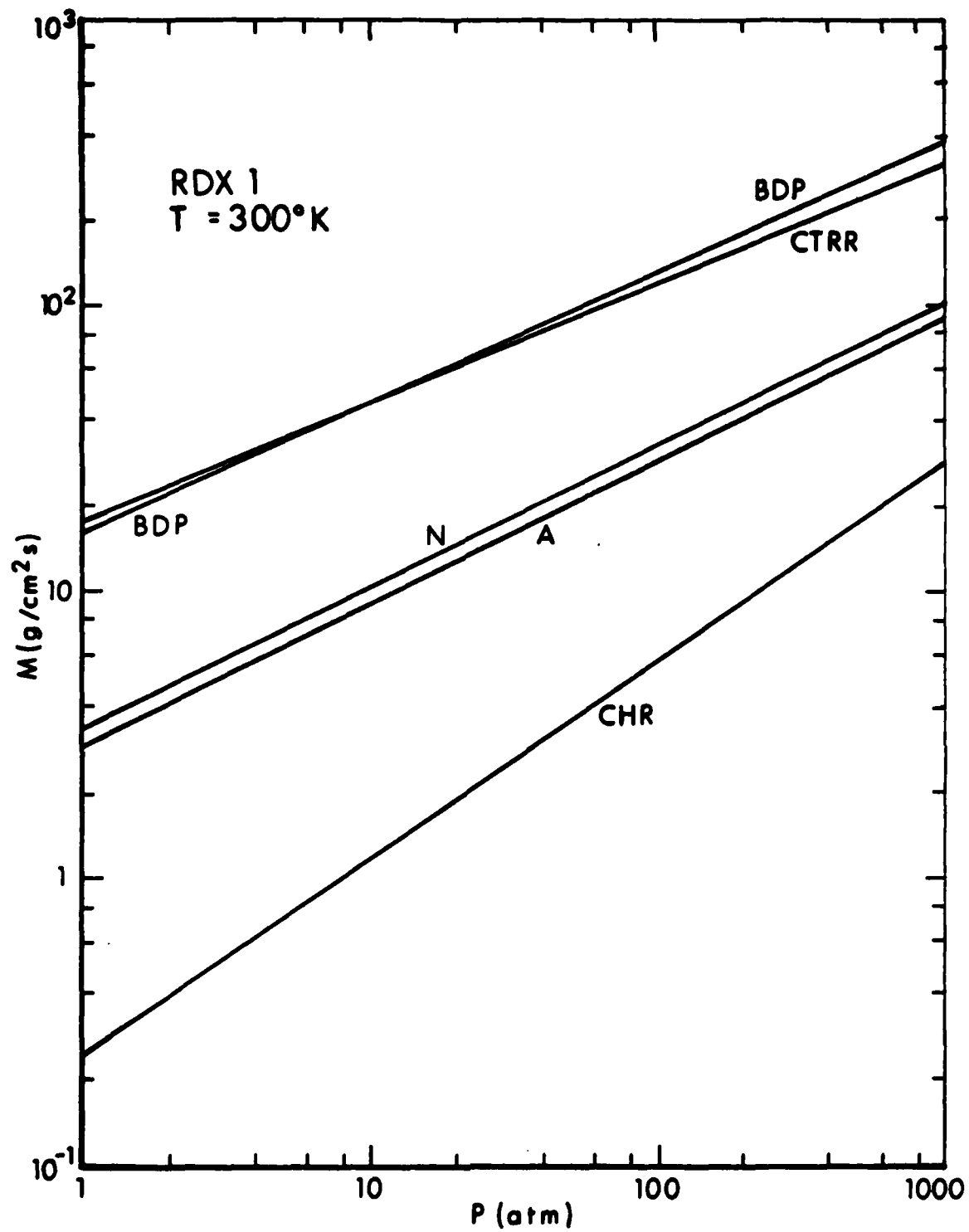


Fig. 14. Mass burning rate vs pressure for RDX1 initially at 300°K.

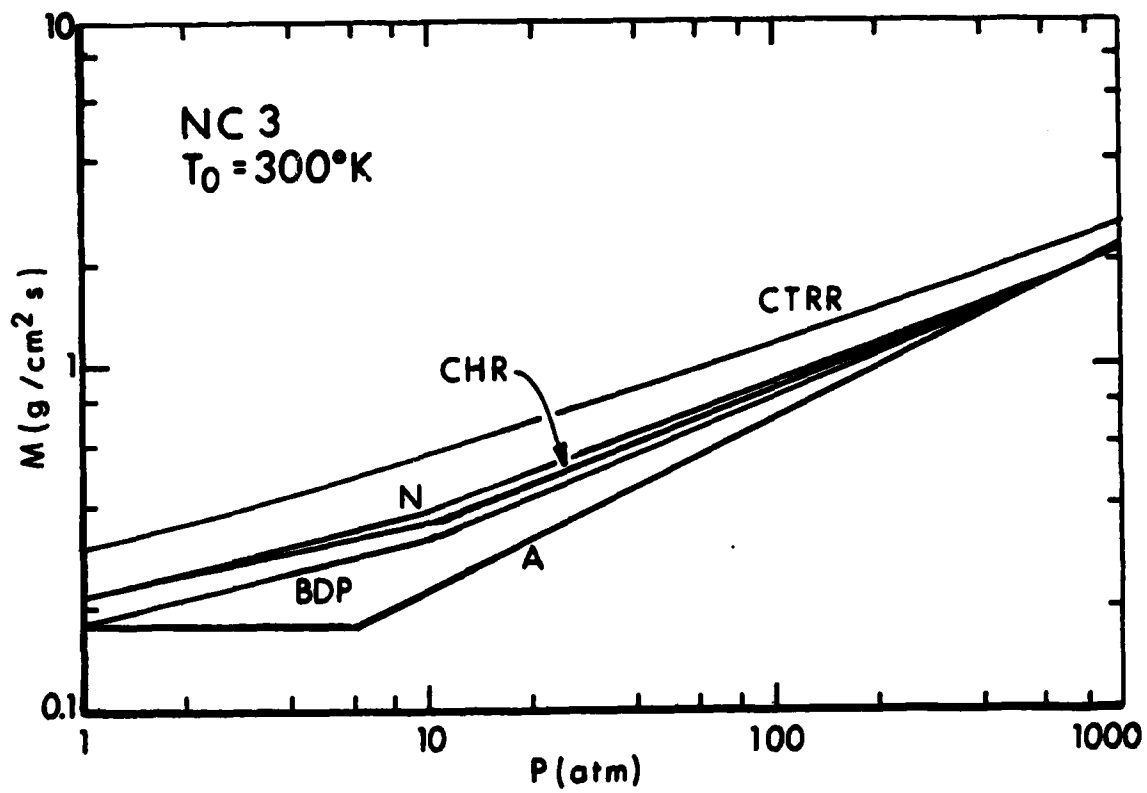


Fig. 15. Mass burning rate vs. pressure for NC3 initially at  $300^\circ\text{K}$ .

in  $T_0$ . Applying Eq. (7) to the asymptotic theory (Eq. (6)) one obtains (cf. Coates<sup>11</sup> Eq. 23)

$$\sigma_p = \left(1 + \frac{v}{2} + \frac{E_G}{2RT_f}\right) / T_f \quad (8)$$

which predicts  $\sigma_p$  to be a monotonic decreasing function of  $T_0$  (since  $T_f = T_0 + Q_T/C_p$ ). The QCHR model<sup>1</sup>, on the other hand, predicts  $\sigma_p$  to increase monotonically with  $T_0$ . Figures 16-21 show the resolution of this conflict. In all of the figures the abrupt transition of the asymptotic theory curve (A) to the solid-phase control limit (given by  $\frac{E_s}{R(T_0 + Q_s/C_p)^2}$ ) does not derive from Eq. (8), but

rather from the condition that the surface temperature cannot drop below  $T^s = T_0 + Q_s/C_p$ . It can also be seen that in the CHR model  $\sigma_p$  does decrease with increasing  $T_0$  at sufficiently low  $T_0$ . This behavior contradicts the QCHR formula derived in Ref. 1 even though most of the conditions for the derivation are satisfied. The discrepancy can be traced to the fact that the QCHR formula was based on a neglect of diffusion.

Figures 18 and 19 for RDX1 show a slight hump in the numerical  $\sigma_p(T_0)$  curves just to the left of the minimum. The numerical integrations were recomputed in this region with increased accuracy for the 1 atm case. The hump remained, indicating that it is apparently not an artifact of the numerical method.

Although the abscissa in Figs. 12-17 is given as  $T_0$ , it could also be  $(T_0 + Q_s/C_p)$  with equal validity since  $Q_s$  is fixed for each of the data sets. However if one assumes  $T_0$  to be fixed and increases in the abscissa to be due to higher  $Q_s$ , one sees that the consequences for  $\sigma_p$  depend on the data set. For example increasing  $Q_s$  by 50 cal/gm would decrease  $\sigma_p$  over the practical range for the RDX1 data set but increase  $\sigma_p$  for the NC3 case (at 1000 atm). Thus it would seem that if combustion models were looked to for guidance in making formulation changes to affect  $\sigma_p$ , a determination of the effective kinetic parameters for the unmodified propellant is first required.

#### IV. CONCLUSIONS

The objective of this study was to assess the numerical accuracy of the computational algorithms employed by several combustion models by direct comparison with accurate numerical solutions of the conservation equations. This comparison was made for a number of data sets with widely varying kinetics parameters. None of the algorithms were found to give reliable numerical accuracy for all data sets and conditions of pressure and temperature. Such inaccuracies can confuse efforts to associate idealized combustion mechanisms with real propellants and give erroneous guidance for performance tailoring attempts.

<sup>11</sup> Coates, R.L., "An Analysis of a Simplified Laminar Flame Theory for Solid Propellant Combustion," *Comb. Sci. Tech.*, Vol. 4, pp. 1-8, 1971.

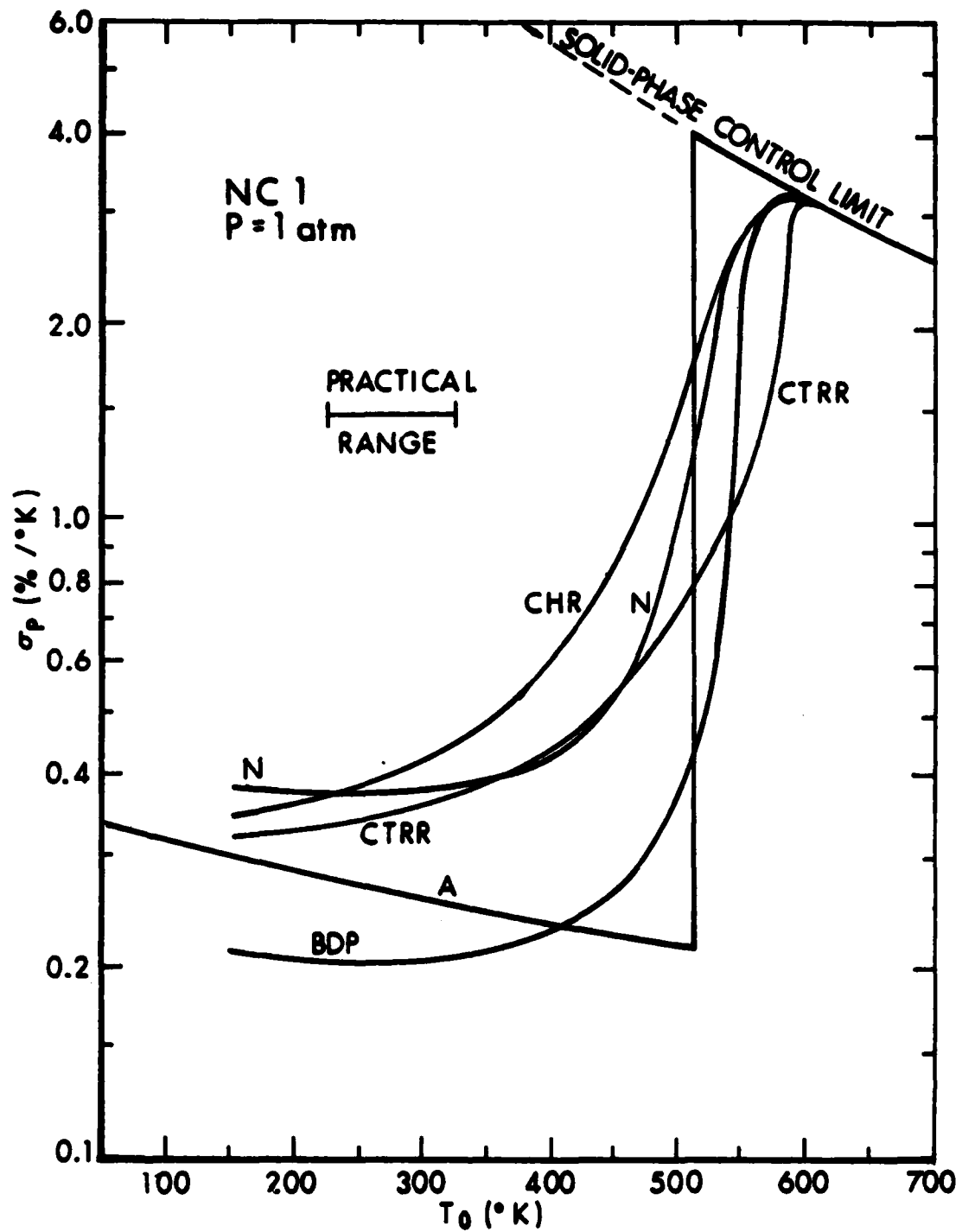


Fig. 16. Temperature sensitivity vs. initial temperature for NCl at 1 atm.

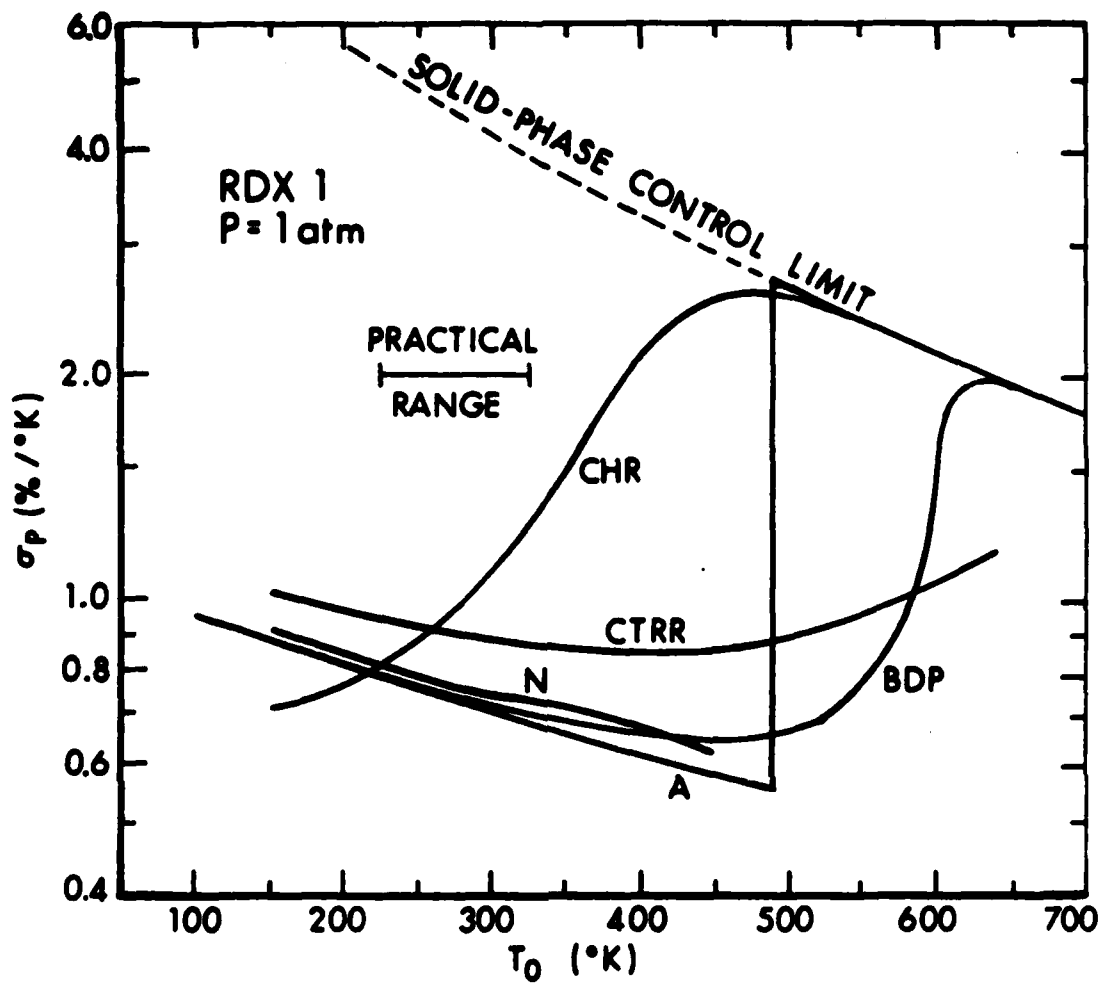


Fig. 18. Temperature sensitivity vs. initial temperature for RDX1 at 1 atm.

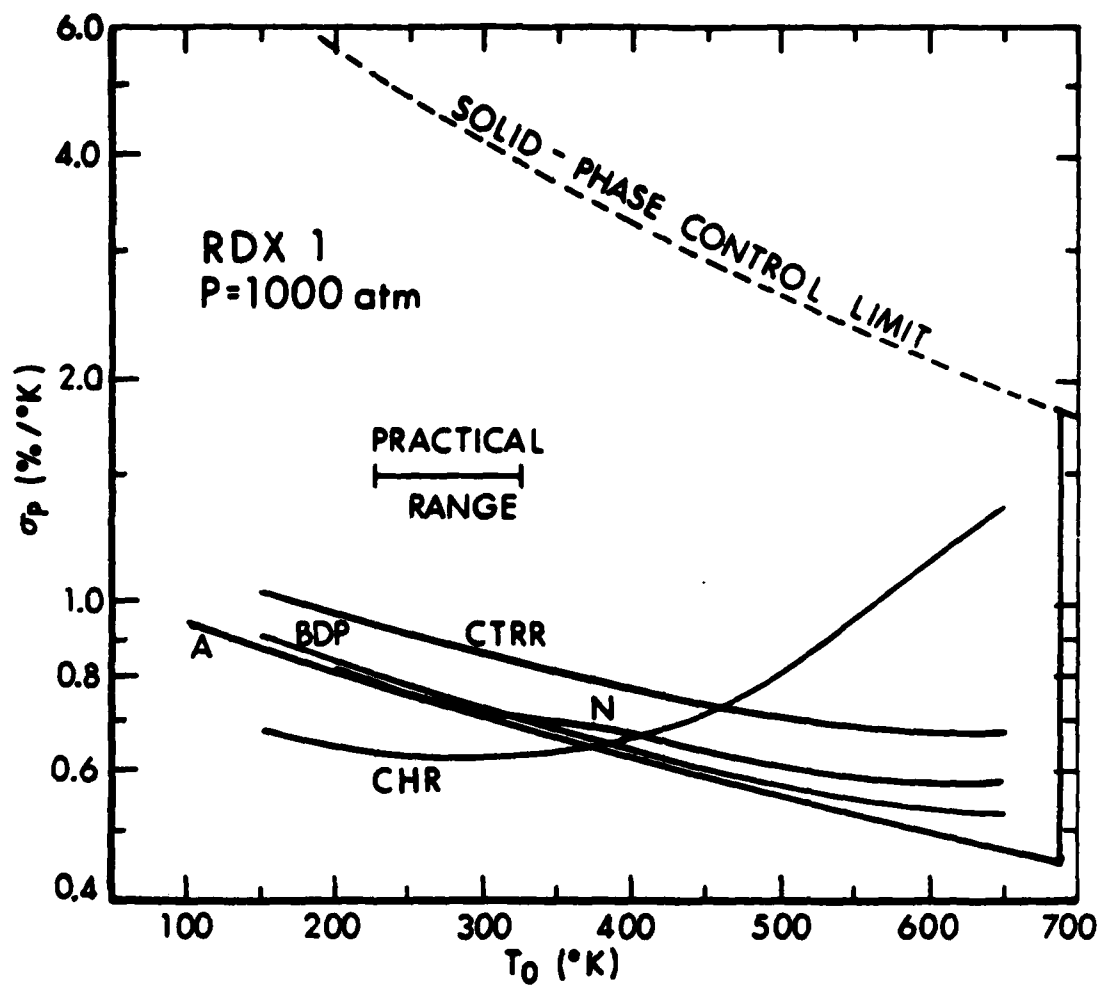


Fig. 19. Temperature sensitivity vs. initial temperature for RDX1 at 1000 atm.

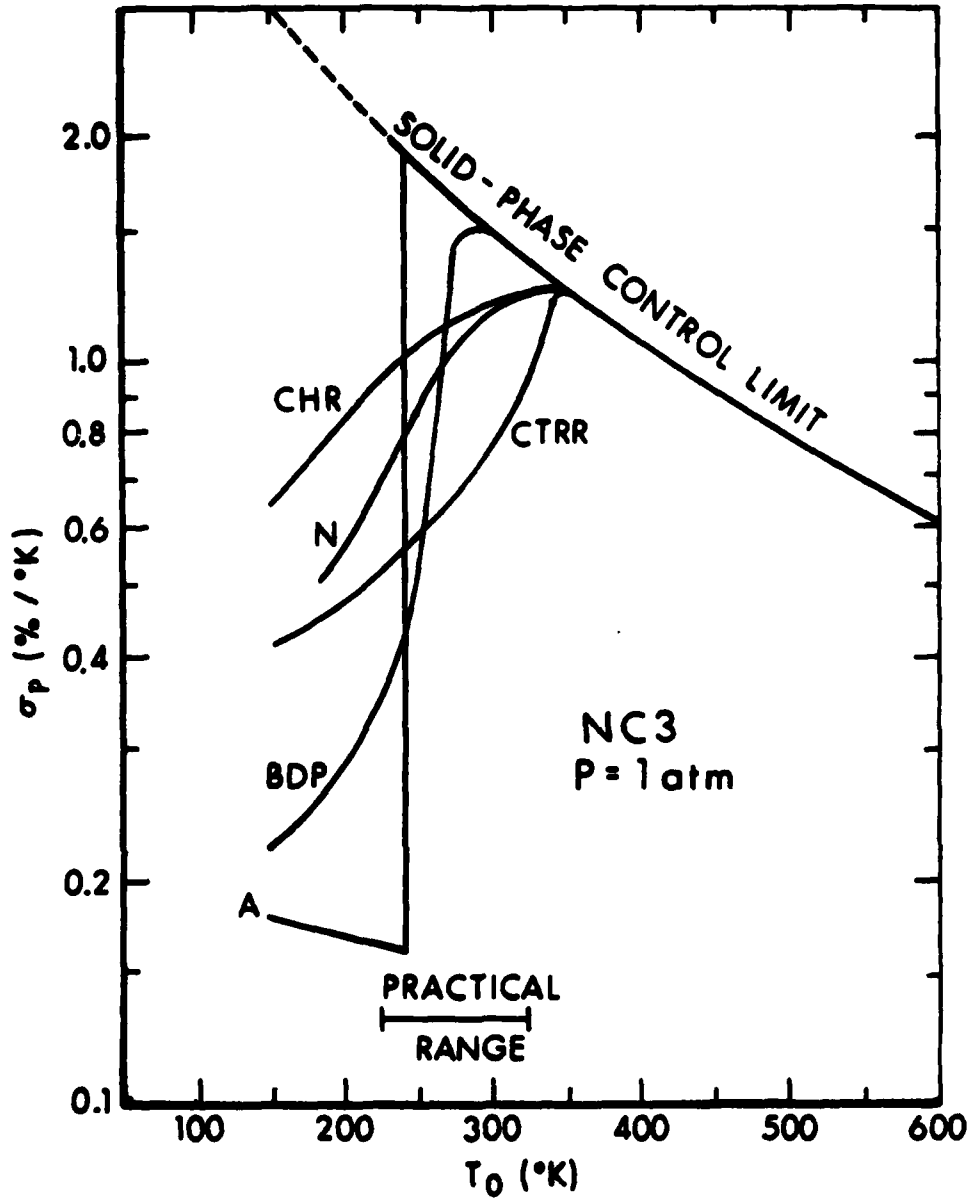


Fig. 20. Temperature sensitivity vs. initial temperature for NC3 at 1 atm.

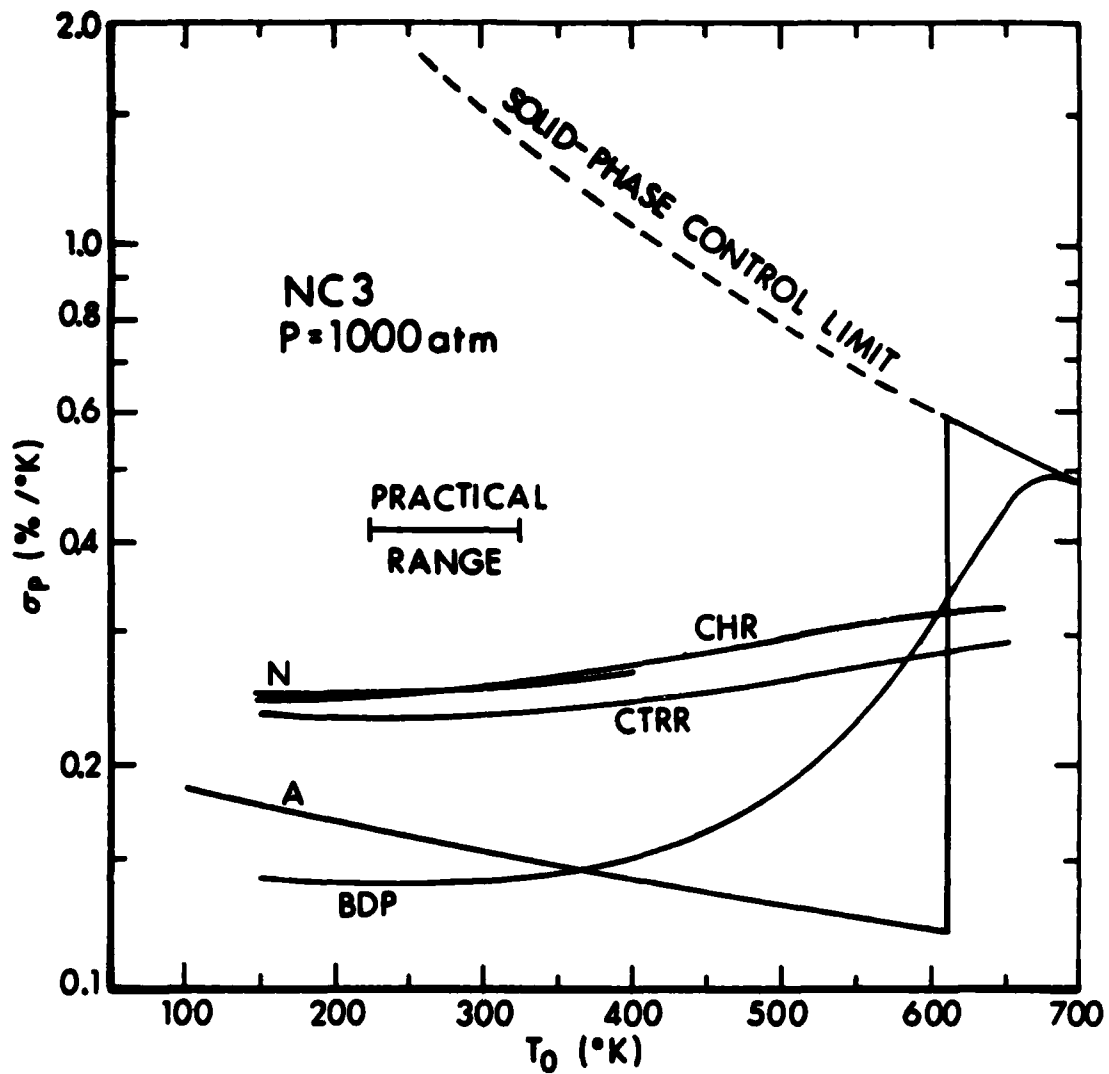


Fig. 21. Temperature sensitivity vs. initial temperature for NC3 at 1000 atm.

In spite of the poor reliability of these algorithms in general, some of the models were shown to give accurate results under certain limiting conditions. However, quantitative criteria for identifying these limits may be difficult to establish for a priori use.

Finally, we have reported numerical calculations of gas-phase heat feedback for a wide range of kinetics parameters. It is hoped that future algorithm developers will find in them a ready means for validating their efforts.

## REFERENCES

1. Miller, M.S., "In Search of an Idealized Model of Homogeneous Solid Propellant Combustion," Combustion and Flame, Vol. 46, pp. 51-73, 1982.
2. Miller, M.S., and Coffee, T.P., "A Fresh Look at the Classical Approach to Solid Propellant Combustion Modeling," to be published in Combustion and Flame.
3. Coffee, T.P. and Heimerl, J.M., "A Method for Computing the Flame Speed for a Laminar, Premixed, One Dimensional Flame," Ballistic Research Laboratory Technical Report ARBRL-TR-02212, January 1980. AD A082803
4. Coffee, T.P., "A Computer Code for the Solution of the Equations Governing a Laminar, Premixed, One Dimensional Flame," Ballistic Research Laboratory Memorandum Report No. ARBRL-MR-03165, April 1982. AD A114041
5. Madsen, N.K. and Sinovec, R.F., "PDECOL, General Collocation Software for Partial Differential Equations," ACM TOMS, Vol. 5, pp. 326-351, 1979.
6. Beckstead, M.W., Derr, R.L., and Price, C.E., "The Combustion of Solid Monopropellants and Composite Propellants," Thirteenth Symposium (International) on Combustion, The Combustion Institute, 1971, pp. 1047-1056.
7. Hermance, C.E., "A Model of Composite Propellant Combustion Including Surface Heterogeneity and Heat Generation," AIAA Journal, Vol. 4, pp. 1629-1637, 1966.
8. Williams, F.A., "Quasi-Steady Gas-Flame Theory in Unsteady Burning of a Homogeneous Solid Propellant," AIAA Journal, Vol. 11, pp. 1328-1330, 1973.
9. Buckmaster, J.D., Kapila, A.K., and Ludford, G.S.S., "Linear Condensate Deflagration for Large Activation Energy," Acta Astronautica, Vol. 3, pp. 593-614, 1976.
10. Bush, W.B., and Fendell, F.E., "Asymptotic Analysis of Laminar Flame Propagation for General Lewis Numbers," Comb. Sci. Tech., Vol. 1, pp. 421-428, 1970.
11. Coates, R.L., "An Analysis of a Simplified Laminar Flame Theory for Solid Propellant Combustion," Comb. Sci. Tech., Vol. 4, pp. 1-8, 1971.

## LIST OF SYMBOLS

- A - propellant molecule label
- $A_G$  - gas-phase reaction frequency factor
- B - gas-phase reactant label
- C - gas-phase product label
- $C_p$  - specific heat for solid and gas phases
- D - diffusion coefficient
- $E_G$  - activation energy for gas-phase reaction
- $E_s$  - activation energy for solid-phase reaction
- M - mass regression rate (mass flux)
- $M_0$  - constant in pyrolysis surface decomposition mechanism
- $m_B^{-0}$ ,  $m_B^{+0}$  - mass fraction of B evaluated at negative and positive sides of the solid/gas interface, respectively.
- $N_2$  - number of moles of C produced per mole of B which reacts
- P - total pressure
- $Q_s$  - heat of reaction per unit mass for solid reaction (positive for exothermic)
- $Q_G$  - exothermic gas-phase reaction heat per unit mass of B
- $Q_T$  - total exothermic reaction heat (solid + gas) per unit mass of A
- $q(x)$  - gas-phase heat release per unit volume per unit time at x
- $q_0$  - value of the heat release function at the surface
- R - universal gas constant
- $R(x)$  - mass of B reacting per unit volume per unit time at x
- $R_0$  - constant mass reaction rate in Constant Temperature Reaction Rate model
- r - linear regression rate of propellant surface
- T, T(x) - temperature at x
- $T_0, T_s, T_f$  - initial, surface, and flame temperatures, respectively
- $\bar{W}$  - average molecular weight of mixture in gas-phase
- x - spatial variable

LIST OF SYMBOLS (Cont'd)

$\lambda$  - heat conductivity in gas-phase

$\nu$  - gas-phase reaction order

$\rho$  - local mass density in gas-phase

$\sigma_p$  - temperature sensitivity at constant pressure

$\phi_G$  - heat flux from gas phase to surface supplied by gas-phase heat release

$\phi_s$  - heat flux from gas phase required by solid to maintain steady-state regression

DISTRIBUTION LIST

<u>No. of Copies</u>	<u>Organization</u>	<u>No. of Copies</u>	<u>Organization</u>
12	Administrator Defense Technical Info Center ATTN: DTIC-DDA Cameron Station Alexandria, VA 22314	4	Commander U.S. Army Research Office ATTN: D. Squire R. Singleton D. Mann R. Girardelli Research Triangle Park, NC 27709
1	Commander US Army Materiel Development and Readiness Command ATTN: DRCDMD-ST 5001 Eisenhower Avenue Alexandria, VA 22333	1	Commander US Army Communications Rsch and Development Command ATTN: DRDCO-PPA-SA Fort Monmouth, NJ 07703
1	Commander US Army Armament Research and Development Command ATTN: DRDAR-TDC (D. Gyorog) Dover, NJ 07801	1	Commander US Army Electronics Research and Development Command Technical Support Activity ATTN: DELSD-L Fort Monmouth, NJ 07703
1	Commander US Army Armament Materiel and Readiness Command ATTN: DRSAR-LEP-L, Tech Lib Rock Island, IL 61299	4	Commander US Army Armament Research and Development Command ATTN: DRDAR-LCA-G D. S. Downs J. Lannon DRDAR-TSS (2 Cys) Dover, NJ 07801
1	Director US Army Armament Research and Development Command Benet Weapons Laboratory ATTN: DRDAR-LCB-TL Watervliet, NY 12189	1	Commander US Army Armament Research and Development Command ATTN: L. Stiefel/DRDAR-SCA-T Dover, NJ 07802
1	Commander US Army Aviation Research and Development command ATTN: DRDAV-E 4300 Goodfellow Blvd St. Louis, MO 63120	3	Commander US Army Missile Command ATTN: DRSMI-YDL DRSMI-RK, D.J. Ifshin DRSNI-R Redstone Arsenal, AL 35898
1	Director US Army Air Mobility Research and Development Laboratory Ames Research Center Moffett Field, CA 94035		

DISTRIBUTION LIST

<u>No. of Copies</u>	<u>Organization</u>	<u>No. of Copies</u>	<u>Organization</u>
1	Commander US Army Tank Automotive Rsch and Development Command ATTN: DRDTA-UL Warren, MI 48090	2	Commander Naval Weapons Center ATTN: Ronald L. Derr Code 388 T. Boggs China Lake, CA 93555
1	Director US Army TRADOC System Analysis Activity ATTN: ATAA-SL, Tech Lib White Sands Missile Range NM 88002	4	Commander Naval Research Laboratory ATTN: J. McDonald L. Harvey E. Orin J. Shnur Washington, DC 20375
1	Office of Naval Research ATTN: R.S. Miller Code 473 800 N. Quincy Street Arlington, VA 22217	1	Commanding Officer Naval Underwater Systems Center Weapons Dept. ATTN: R.S. Lazar, Code 36301 Newport, RI 02840
1	Navy Strategic Systems Project Office ATTN: Roy D. Kinert, SP 2731 Washington, DC 20376	1	Superintendent Naval Postgraduate School Department of Aeronautics ATTN: D.W. Netzer Monterey, CA 93940
1	Naval Air Systems Command ATTN: J. Ramnarace, AIR-54111C Washington, DC 20360	5	AFRPL (DRSC) ATTN: D. George J.N. Levine W. Roe R. Geisler B. Goshgarian Edwards AFB, CA 93523
3	Commander Naval Ordnance Station ATTN: Peter L. Stang, Steve Mitchell Charles Irish Indian Head, MD 20640	1	AFATL/DLDD ATTN: O.K. Heiney Eglin AFB, FL 32542
1	Commander Naval Surface Weapons Center ATTN: Jesse L. East, Jr. Dahlgren, VA 22448	1	AFOSR ATTN: L.H. Caveny Bolling Air Force Base Washington, DC 20332
1	Commander Naval Surface Weapons Center ATTN: G.B. Wilmot/R16 Silver Spring, MD 20910	1	Aerojet Solid Propulsion Co. ATTN: P. Micheli Sacramento, CA 95813

DISTRIBUTION LIST

<u>No. of Copies</u>	<u>Organization</u>	<u>No. of Copies</u>	<u>Organization</u>
1	AVCO Everett Rsch Lab Div ATTN: D. Stickler 2385 Revere Beach Parkway Everett, MA 02149	1	Hercules, Inc. Bacchus Works ATTN: K.P. McCarty P.O. Box 98 Magna, UT 84044
1	Applied Combustion Tech., Inc. ATTN: A. Michael Varney 2910 N. Orange Ave. Orlando, FL 32804	1	Hercules, Inc. Eglin Operations AFATL/DLDD ATTN: R.L. Simmons Eglin AFB, FL 32542
2	Atlantic Research Corp. ATTN: M.K. King 5390 Cherokee Ave Alexandria, VA 22314	1	Honeywell, Inc. Govt & Aerospace Products Div ATTN: D.E. Broden 600 2nd Street NE Hopkins, MN 55343
1	Battelle-Columbus Labs Tactical Technology Center ATTN: J. Huggins 505 King Avenue Columbus, OH 43201	1	NASA Langley Research Center ATTN: G.B. Northam/MS 168 Hampton, VA 23365
1	Calspan Corporation ATTN: E.B. Fisher P.O. Box 400 Buffalo, NY 14225	1	Lawrence Livermore National Laboratory ATTN: C. Westbrook Livermore, CA 94550
1	Ford Aerospace & Communications Corp. ATTN: D. Williams Main Street Ford Road Newport Beach, CA 92663	1	Lockheed Missiles & Space Company ATTN: George Lo 3251 Hanover St., Dept. 52- 35/B204/2 Palto Alto, CA 94304
1	General Electric Co Armament Department ATTN: M.J. Bulman Lakeside Avenue Burlington, VT 05402	2	Los Alamos National Lab Center for Non-Linear Studies ATTN: B. Nichols L. Warner P.O. Box 1663 Los Alamos, NM 87545
1	General Electric Company ATTN: Marshall Lapp Schenectady, NY 12301	1	National Bureau of Standards ATTN: T. Kashiwagi Washington, DC 20234
1	Hercules Powder Co. Allegheny Ballistics Lab ATTN: R.R. Miller P.O. Box 210 Cumberland, MD 21501	1	Norman Cohen Prof Services 105 Summit Ave Redlands, CA 92373

DISTRIBUTION LIST

<u>No. of Copies</u>	<u>Organization</u>	<u>No. of Copies</u>	<u>Organization</u>
1	Olin Corporation Smokeless Powder Operations ATTN: R.L. Cook P.O. Box 222 St. Marks, FL 32355	4	SRI International ATTN: Tech Lib S. Barker D. Crosley D. Golden 333 Ravenswood Avenue Menlo Park, CA 94025
1	Paul Gough Associates, Inc. ATTN: P.S. Gough P.O. Box 1614 Portsmouth, NH 03801	1	Stevens Institute of Tech Davidson Laboratory ATTN: R. McAlevy, III Hoboken, NJ 07030
2	Princeton Combustion Rsch Labs ATTN: M. Summerfield N.A. Messina 1041 U.S. Highway One North Princeton, NJ 08540	1	Teledyne McCormack-Selph ATTN: C. Leveritt 3601 Union Rd Hollister, CA 95023
1	Pulsepower Systems, Inc. ATTN: L.C. Elmore 815 American Street San Carlos, CA 94070	1	Thiokol Corporation Elkton Division ATTN: W.N. Brundige P.O. Box 241 Elkton, MD 21921
1	Rockwell International Corp Rocketdyne Division ATTN: J.E. Flanagan/BA17 6633 Canoga Avenue Canoga Park, CA 91304	1	Thiokol Corporation Huntsville Division ATTN: D.A. Flanagan Huntsville, AL 35807
1	Science Applications, Inc. ATTN: R.B. Edelman 23146 Cumorah Crest Woodland Hills, CA 91364	1	Thiokol Corporation Wasatch Division ATTN: J.A. Peterson P.O. Box 524 Brigham City, UT 84302
1	Science Applications, Inc. ATTN: H.S. Pergament 1100 State Road, Bldg. N Princeton, NJ 08540	2	United Technologies Chemical Systems Div ATTN: R. Brown R. McLaren P. O. Box 358 Sunnyvale, CA 94086
1	Shock Hydrodynamics ATTN: W. Anderson 4710-16 Vineland Ave N. Hollywood, CA 91602	1	Universal Propulsion Co ATTN: H.J. McSpadden Black Canyon Stage 1 Box 1140 Phoenix, AZ 85029
1	Space Sciences, Inc. ATTN: M. Farber Monrovia, CA 91016		

DISTRIBUTION LIST

<u>No. of Copies</u>	<u>Organization</u>	<u>No. of Copies</u>	<u>Organization</u>
1	Brigham Young University Department of Chemical Engineering ATTN: M.W. Beckstead Provo, Ut 84601	3	Georgia Institute of Technology School of Aerospace Engineering ATTN: B.T. Zinn E. Price W.C. Strahle Atlanta, GA 30332
2	California Institute of Technology Jet Propulsion Laboratory ATTN: L.D. Strand 4800 Oak Grove Drive Pasadena, CA 91103	1	Hughes Aircraft Co ATTN: T.E. Ward 8433 Fallbrook Ave Canoga Park, CA 91303
1	California Institute of Technology ATTN: F.E.C. Culick 204 Karman Lab Pasadena, CA 91125	1	University of Illinois Dept of Mech Eng ATTN: H. Krier 144 MEB, 1206 W Green St. Urbana, IL 61801
1	University of S. California Dept of Chemistry ATTN: S. Benson Los Angeles, CA 90007	1	Johns Hopkins Univ/APL Chemical Propulsion Info Agency ATTN: T.W. Christian Johns Hopkins Road Laurel, MD 20707
1	University of California Los Alamos National Lab ATTN: T.D. Butler P.O. Box 1663, Mail Stop 216 Los Alamos, NM 87545	1	University of Minnesota Dept of Mechanical Engineering ATTN: E. Fletcher Minneapolis, MN 55455
1	University of California Berkeley Mechanical Engineering Dept ATTN: J. Daily Berkeley, CA 94720	2	Southwest Research Institute ATTN: A.B. Wenzel W.H. McLain 8500 Culebra Rd. San Antonio, TX 78228
1	Case Western Reserve Univ. Division of Aerospace Sciences ATTN: J. Tien Cleveland, OH 44135		
1	Energy Research Lab United Technologies Rsch Center ATTN: A.C. Eckbreth East Hartford, CT 06504		

DISTRIBUTION LIST

<u>No. of Copies</u>	<u>Organization</u>
4	Pennsylvania State University Applied Research Laboratory ATTN: K.K. Kuo G.M. Faeth H. Palmer M. Micci P.O. Box 30 University Park, PA 16802
1	Princeton University Forrestal Campus Library ATTN: F.A. Williams P.O. Box 710 Princeton, NJ 08540
2	Purdue University School of Aeronautics and Astronautics ATTN: J.R. Osborn R. Glick Grissom Hall West Lafayette, IN 47907
2	University of Texas Dept of Chemistry ATTN: W. Gardiner H. Schafer Austin, TX 78712
1	University of Utah Dept of Chemical Engineering ATTN: G. Flandro Salt Lake City, UT 84112
1	Virginia Polytechnical Inst. State Univ. ATTN: J.A. Schetz Blacksburg, VA 24061

Aberdeen Proving Ground

Dir, USAMSAA  
ATTN: DRXSY-D  
DRXSY-MP, H. Cohen  
Cdr, USATECOM  
ATTN: DRSTE-TO-F  
Dir, USACSL, Bldg. E3516, EA  
ATTN: DRDAR-CLB-PA

USER EVALUATION OF REPORT

Please take a few minutes to answer the questions below; tear out this sheet, fold as indicated, staple or tape closed, and place in the mail. Your comments will provide us with information for improving future reports.

1. BRL Report Number \_\_\_\_\_

2. Does this report satisfy a need? (Comment on purpose, related project, or other area of interest for which report will be used.)

\_\_\_\_\_  
\_\_\_\_\_  
\_\_\_\_\_

3. How, specifically, is the report being used? (Information source, design data or procedure, management procedure, source of ideas, etc.) \_\_\_\_\_

\_\_\_\_\_  
\_\_\_\_\_

4. Has the information in this report led to any quantitative savings as far as man-hours/contract dollars saved, operating costs avoided, efficiencies achieved, etc.? If so, please elaborate.

\_\_\_\_\_  
\_\_\_\_\_

5. General Comments (Indicate what you think should be changed to make this report and future reports of this type more responsive to your needs, more usable, improve readability, etc.) \_\_\_\_\_

\_\_\_\_\_  
\_\_\_\_\_  
\_\_\_\_\_

6. If you would like to be contacted by the personnel who prepared this report to raise specific questions or discuss the topic, please fill in the following information.

Name: \_\_\_\_\_

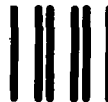
Telephone Number: \_\_\_\_\_

Organization Address: \_\_\_\_\_

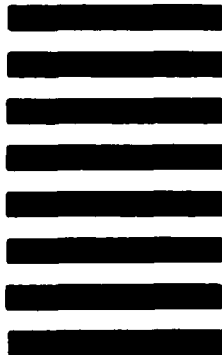
\_\_\_\_\_  
\_\_\_\_\_

FOLD HERE

Director  
US Army Ballistic Research Laboratory  
Aberdeen Proving Ground, MD 21005



NO POSTAGE  
NECESSARY  
IF MAILED  
IN THE  
UNITED STATES



OFFICIAL BUSINESS  
PENALTY FOR PRIVATE USE, \$300

**BUSINESS REPLY MAIL**  
FIRST CLASS PERMIT NO 12062 WASHINGTON, DC  
POSTAGE WILL BE PAID BY DEPARTMENT OF THE ARMY

Director  
US Army Ballistic Research Laboratory  
ATTN: DRDAR-TSB-s  
Aberdeen Proving Ground, MD 21005

FOLD HERE